1-1-2017

Astrocytes promote progression of breast cancer metastases to the brain via a KISS1-mediated autophagy.

Natalya Kaverina

Anton V Borovjagin

Zaira Kadagidze

Anatoly Baryshnikov

Maria Baryshnikova

See next page for additional authors

Authors
Natalya Kaverina, Anton V Borovjagin, Zaira Kadagidze, Anatoly Baryshnikov, Maria Baryshnikova, Dmitry Malin, Dhimankrishhna Ghosh, Nameeta Shah, Danny R Welch, Patrik Gabikian, Apollon Karseladze, Charles Cobbs, and Ilya V Ulasov

AUTOPHAGY
2017, VOL. 13, NO. 11, 1905–1923
https://doi.org/10.1080/15548627.2017.1360466

Taylor & Francis
Taylor & Francis Group

RESEARCH PAPER-BASIC SCIENCE

Astrocytes promote progression of breast cancer metastases to the brain via a KISS1-mediated autophagy

Natalya Kaverina[a], Anton V. Borovjagin[b], Zaira Kadagidze[a], Anatoly Baryshnikov[c], Maria Baryshnikova[c], Dmitry Malin[d,e], Dhimankrishhna Ghosh[f], Nameeta Shah[f], Danny R. Welch[g], Patrik Gabikian[h], Apollon Karseladze[i], Charles Cobbs[e], and Ilya V. Ulasov[f,j]

[a]Department of Tumor Immunology, Institute of Experimental Diagnostics and Therapy of Tumors, N.N. Blokhin Cancer Research Center, Moscow, Russia; [b]University of Alabama at Birmingham School of Dentistry, Institute of Oral Health Research, Birmingham, AL, USA; [c]Institute of Experimental Diagnostics and Therapy of Tumors, N.N. Blokhin Cancer Research Center, Moscow, Russia; [d]Department of Endocrinology, University of Wisconsin-Madison, Madison, WI, USA; [e]Laboratory of Psychiatric Neurobiology, Institute of Molecular Medicine, Sechenov First Moscow State Medical University, Moscow, Russia; [f]Center for Advanced Brain Tumor Treatment, Swedish Neuroscience Institute, Seattle, WA, USA; [g]Department of Cancer Biology, Kansas University Medical Center (KUMC), Kansas City, KS, USA; [h]Department of Neurosurgery, Kaiser Permanente Los Angeles Medical Center, Los Angeles, CA, USA; [i]Pathology, Institute of Experimental Diagnostics and Therapy of Tumors, N.N. Blokhin Cancer Research Center, Moscow, Russia; [j]Institute of Molecular Medicine, Sechenov First Moscow State Medical University, Moscow, Russia

ABSTRACT

Formation of metastases, also known as cancer dissemination, is an important stage of breast cancer (BrCa) development. *KISS1* expression is associated with inhibition of metastases development. Recently we have demonstrated that BrCa metastases to the brain exhibit low levels of KISS1 expression at both mRNA and protein levels. By using multicolor immunofluorescence and coculture techniques here we show that normal adult astrocytes in the brain are capable of promoting metastatic transformation of circulating breast cancer cells localized to the brain through secretion of chemokine CXCL12. The latter was found in this study to downregulate *KISS1* expression at the post-transcriptional level via induction of microRNA-345 (*MIR345*). Furthermore, we demonstrated that ectopic expression of *KISS1* downregulates *ATG5* and *ATG7*, 2 key modulators of autophagy, and works concurrently with autophagy inhibitors, thereby implicating autophagy in the mechanism of *KISS1*-mediated BrCa metastatic transformation. We also found that expression of *KISS1* in human breast tumor specimens inversely correlates with that of MMP9 and IL8, implicated in the mechanism of metastatic invasion, thereby supporting the role of KISS1 as a potential regulator of BrCa metastatic invasion in the brain. This conclusion is further supported by the ability of KISS1, ectopically overexpressed from an adenoviral vector in MDA-MB-231Br cells with silenced expression of the endogenous gene, to revert invasive phenotype of those cells. Taken together, our results strongly suggest that human adult astrocytes can promote brain invasion of the brain-localized circulating breast cancer cells by upregulating autophagy signaling pathways via the CXCL12-*MIR345*-KISS1 axis.

ARTICLE HISTORY
Received 23 December 2015
Revised 7 July 2017
Accepted 24 July 2017

KEYWORDS
autophagy; brain metastases; breast cancer; KISS1 suppressor; stem cells

Introduction

Breast cancer (BrCa) is the most common primary malignancy of women, accounting for almost 30% of all female cancers worldwide. Breast cancer mortality is associated with the dissemination of cancer cells to multiple organs such as lungs, bones and brain.[1] The mechanism of BrCa dissemination is complex and involves several genes,[2] some of which serve as mediators, while others as suppressors[3] of metastasis. Among the suppressors, the *KISS1/kisspeptin 1* (KiSS-1 metastasis-suppressor) gene deserves special attention. This gene encodes a 145-amino acid (aa) precursor peptide that becomes cleaved into several short peptides of 10^4-, 13- and 14 aa in length. KISS1 inhibits growth and invasion of osteosarcoma[5] and prostate cancer cells.[6]

Whereas deficiency of KISS1 expression in tumor tissues is associated with cancer progression,[7] overexpression of this protein can suppresses the formation of metastases[8] via molecular mechanisms involving KISS1R[9] and CXCR4[10] receptors. Although, our group[11] and others[12] have found a significant reduction in KISS1 expression in BrCa metastases to the brain relative to primary BrCa tumors, the precise role of *KISS1* in the development and progression of brain metastases remains unknown. The objective of this study was to investigate the role of *KISS1* in modulating brain metastases and to reveal the upstream and the downstream effectors of *KISS1* downregulation.

Development of brain metastases is a result of complex interplay between the tumor cells and the tumor environment,[13] which is represented predominantly by normal astrocytes in the brain tissue. Astrocytes regulate the brain response to inflammation,[14] maintain brain homeostasis[15] and provide protection of neurons from hypoxia.[16] Conversely, reactive

CONTACT Ilya V. Ulasov Ilya.Ulasov@Swedish.org; Ulasov75@yahoo.com; Swedish Neuroscience Institute, 550 17th Avenue, Seattle, WA 98122, USA.
Supplemental data for this article can be accessed on the publisher's website.

astrocytes can play a mitogenic role by secreting interleukins and chemokines, such as CCL2 and CXCL12/SDF1, respectively. The latter can serve as a chemoattractant for highly metastatic CXCR4$^+$ cells.[17] Elevated levels of CCL2 and CXCL12 expression have also been linked to tumor progression and development of metastases.[18] Although normal astrocytes have been linked with tumor progression,[14] the role of these cells in brain metastases is still unclear. Here we provide the first evidence that normal astrocytes can promote brain metastases through downregulation of KISS1 and activation of the autophagy survival pathway in circulating BrCa cells.

Results

Primary tumors release KISS1-expressing cancer stem cells into the bloodstream

BrCa is represented by highly heterogeneous tumor types,[19] each containing a distinctive population of cancer cells with stem cell properties,[20] resistance to conventional BrCa therapies,[21] and capability of migrating[22] and initiating metastases in the brain. We hypothesized that blood-circulating cancer stem cells (CSC) with a self-renewal property and a KISS1-deficient phenotype could give rise to metastatic foci in the brain. To identify and isolate a population of circulating tumor cells (CTCs), we used a previously described[23] MDA-MB-231 metastatic model of human BrCa in mice.[24] We observed a strong association between primary tumor growth and number of CTCs in the blood (Fig. S1A to D). Using an in vitro tumorigenicity analysis we showed that CD24$^{-/LOW}$ and CD44$^+$ cells exhibit a ~7.2- and ~1.48-fold higher potential to form tumors as compared with CD24$^+$ and CD44$^+$ or parental cells, respectively (Fig. S1E, $P < 0.05$), which highlights their potential for forming secondary tumors. In addition, flow cytometry together with the ALDEFLUOR assay[25] (Fig. S1F) demonstrate that the CD24$^{-/LOW}$ and CD44$^+$ population of CSCs isolated from blood (CTC) is metabolically active. We also observed that the CD24$^-$ and CD44$^+$ population of CTCs isolated from nude mice with established MDA-MB-231 mammary tumor xenografts exhibits a 4.7-fold higher expression of *KISS1* mRNA (Fig. S1G), compared with parental CSCs ($P < 0.05$). There was, however, no correlation between the *KISS1* mRNA levels and those of the *ST6GALNAC6* gene,[26] implicated in priming BrCa cells to the brain (Fig. S1H).

Cancer stem cells, identified in BrCa brain metastases by CD44, CD24 and FLOT2 markers, express low level of KISS1

Our next step was to characterize expression of KISS1 in a small subset of metastatic cells called cancer stem cells (CSCs), identified by expression of stem cell markers CD44 and CD24[27] in the primary brain metastatic tissue. Given the low expression levels of KISS1 in BrCa brain metastases,[11] we hypothesized that high expression of KISS1 in CTCs entering the brain could be locally modulated by the brain tissue environment. As evident from Fig. 1A, RONC1 and RONC-BM35 tumor specimens are composed of either distinct CD24- or CD44-positive cells, since no overlap in cell populations expressing those surface markers was observed. Therefore, we characterized CD44$^+$ CSC populations expressing FLOT2/ESA1[28] and KISS1. At the onset, we identified a CD44$^+$, FLOT2$^+$ and KISS1$^-$ CSC population that exhibited colocalization of only 2 distinct IF signals (red and green, respectively), resulting in sky blue cell staining, and subsequently looked for subpopulations also positive for KISS1 expression (CD44$^+$, FLOT2$^+$ and KISS1$^+$) by triple IF staining. These experiments revealed cells with "white" colocalization signal (Fig. 1B,C). While the stem cell population in the primary tumors comprised KISS1-positive (KISS1$^+$) subtypes (average 0.95 ± 0.44 per high power field, Fig. 1D), brain metastatic lesions contained mostly KISS1-negative stem cells (average 1.8 ± 0.85 per high power field, Fig. 1D) These data are consistent with our earlier finding that brain metastatic lesions exhibit drastically lower KISS1 expression levels relative to primary BrCa tumors.[11]

Normal human astrocytes downregulate KISS1 in brain metastases via production of CCL2 and CXCL12

At the next step we determined the region in brain that can modulate KISS1 expression. Given the fact that astrocytes are capable of modulating biologic properties and behavior of cancer cells,[12] we hypothesized that they could induce formation of brain metastases through suppression of KISS1 expression among BrCa cells, entering into the brain. For instance, a triple IF staining of brain metastatic specimens for an astrocyte-specific marker GFAP, a stem cell marker, and CD44 and KISS1 showed that CD44$^+$ and KISS1$^+$ BrCa cells tend to lose KISS1 expression (red in Fig. 2A) after coming into direct contact with GFAP-positive astrocytes (green in Fig. 2A). To find out if human adult astrocytes are capable of modulating KISS1 expression in BrCa CTCs, we examined the level of KISS1 expression in GFP-tagged cancer cells (CN34-GFP, CN34Br-GFP, MDA-MB-231Br-GFP and 4T1Br-GFP) by coculturing them with normal human astrocytes (NHA) or human microglia (HM) in vitro (Fig. 2B, C). Although we observed that only parental CN34 BrCa cells upon their coculturing with astrocytes or human microglia induce *KISS1* mRNA ($P < 0.05$), the brain-primed metastatic MDA-MB-231Br, CN34Br or 4T1Br cancer cells exhibited greater level of *KISS1* downregulation (~65%, ~82% and ~52% reduction vs Mock, respectively) as a result of direct contact with astrocytes. This effect was mediated by a 10- to 1000-fold increase in *CXCL1* ($P = 0.02$), *CCL2* ($P = 0.015$) and *CXCL12* ($P = 0.023$) mRNA expression levels in astrocytes (Fig. 2D) induced through contact with the cancer cells. Furthermore, we discovered that KISS1 expression in CN34Br cells gets selectively inhibited by human CXCL12 and CCL2 proteins in a dose-dependent manner (Fig. 2E, $P < 0.05$), which was further confirmed by IF staining (data not shown). While no colocalization was observed for CCL2 and astrocyte-specific GFAP staining (Fig. 2F, left panels), a distinctive colocalization (yellow and orange signal on merged images) was observed for CXCL12 and GFAP markers in brain metastatic tissues (Fig. 2F, right panels), highlighting the clinical significance of CXCL12$^+$ and GFAP$^+$ reactive astrocytes for the survival of patients with BrCa brain metastases after surgery (Fig. 2G). As expected, the presence of CXCL12$^-$ and GFAP$^+$ cells in BrCa brain metastatic tissue associates with longer patient survival (38.75 ± 23.6 vs 104 ± 20.6 days, $P = 0.019$)

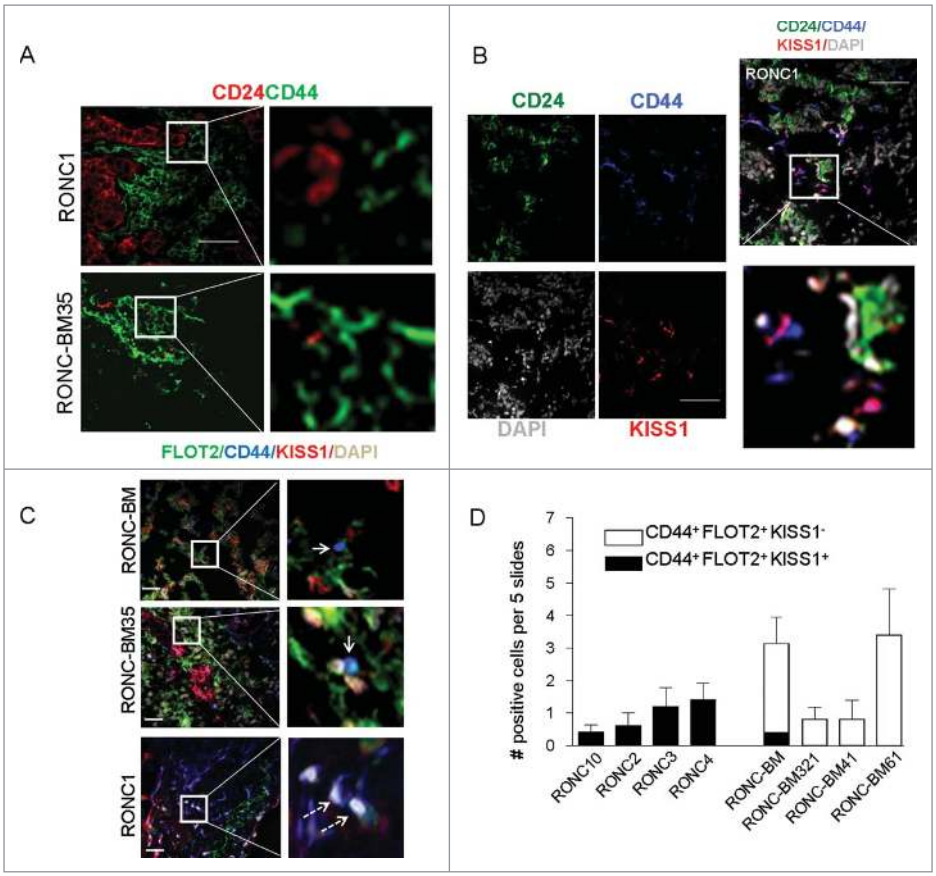

Figure 1. Detection of CSC in the primary BrCa specimens and brain metastatic lesions by immunofluorescence. (A) Double staining of primary BrCa and BrCa metastatic tumors in the brain specimens for stem cell markers CD44 (green membrane staining) and CD24 (red membrane staining) reveals 2 distinct populations of cancer cells (red and green) with no detectable signal colocalization (yellow). (B, C) A 4-color immunostaining reveals loss of KISS1 expression in the BrCa stem cell population of brain metastases. (B) A representative (merged) image (400X, scale bar: 20 μm) showing colocalization of KISS1 with CD44 (magenta signals), but not with CD24 in primary BrCa specimen (RONC1), suggesting that KISS1 is expressed in primary BrCa cells or CSC; KISS1 pseudo-colored with red; CD24 with green; CD44 with blue; and DAPI with gray. (C) Representative (merged) images (400X, scale bar: 20 μm) of brain metastatic tumor (RONC-BM and RONC-BM35) specimens, showing colocalization of CD44 with FLOT2 (sky blue signal indicated by arrow), but not KISS1, in contrast to primary (RONC1) tumors, where CD44 and FLOT2 colocalize with KISS1 resulting in numerous white foci (dashed arrow), not present in metastases; CD44 (blue membrane staining), KISS1 (red cytoplasmic and nuclear staining), DAPI (gray nuclear staining), FLOT2 (green cytoplasmic and membrane staining); Insets (white boxes) show portions of the corresponding images of primary (RONC1, panel B) or metastatic (RONC-BM and RONC-BM35, panel C) tumor specimens at higher magnification. (D) Quantitative assessment of CSC with no KISS1 expression ($CD44^+$, $FLOT2^+$ and $KISS1^-$, sky blue) and KISS1-positive ($CD44^+$, $FLOT2^+$ and$KISS1^+$, white foci) CSC in primary and the brain metastatic specimens (white and black bars, respectively). The amount of KISS1-positive and negative CSC was determined in unmatched specimens (primary BrCa, N = 4) and BrCa metastases to the brain (N = 4) by counting sky-blue and white foci of IF signals on merged images. Each tumor type was analyzed in triplicates with 5 high power fields (HPF) ± SD (standard deviation) and minimum 50 cells per slide.

KISS1 mRNA is a direct target for MIR345

It remains unclear how the CXCL12 chemokine, released by astrocytes, modulates KISS1 expression. Since treatment of BrCa cells with CXCL12 has been shown to induce expression of cellular microRNAs,[29] and suppression of CXCL12 has been found to reduce cancer cell metastases,[30] we hypothesized that CXCL12 could induce a *KISS1*-targeting microRNA, silencing expression of *KISS1* mRNA in metastatic BrCa cells (Fig. S2). In line with the above possibility, some experimental data (Ulasov et al., unpublished) indicated to *MIR345* and *MIR146B* as best candidates for the role of post-transcriptional regulators of *KISS1* expression, since their induction inversely correlated with *KISS1* expression levels in primary tumors, based on quantitative PCR analyses of cancer patient samples. Conversely, among 5 candidate miRNAs with predicted ability to bind (base pair to) the 3′ UTR of the human *KISS1* mRNA (TargetScan-based computational analysis), *MIR345* and *MIR146B* were the only ones whose expression in CN34Br and MDA-MB-231Br brain metastatic cells increased in response to treatment with CXCL12 or CCL2 proteins (Fig. 3A). Indeed, CXCL12 was experimentally confirmed to induce the expression of *MIR345* in a dose-dependent manner, whereas Gene Ontology analysis indicated that *MIR345* could potentially modulate a cytokine-mediated signaling pathway (Fig. 3B, $P = 0.0007$, FDR<2%). Thus regulation of *KISS1* expression at post-transcriptional level in response to CXCL12 or CCL2 was assumed and further directly validated by in vitro assays, using cancer cells stably expressing GFP or Luciferase (Luc) reporters, fused to the 3′UTR sequence (bearing potential *MIR345* target site) of the human *KISS1* mRNA. Expression of the reporters was analyzed following treatment of the transfected cells with NHA-conditioned media or individual recombinant CCL2 or CXCL12 proteins (Fig. S3). Alternatively, the reporter gene expression was analyzed following a direct transfection of the cells with human *MIR345–5p* mimic. As expected, treatment with either purified CXCL12 ($P = 0.003$) or *MIR345–5p* mimic ($P = 0.018$) significantly decreased expression of GFP from the

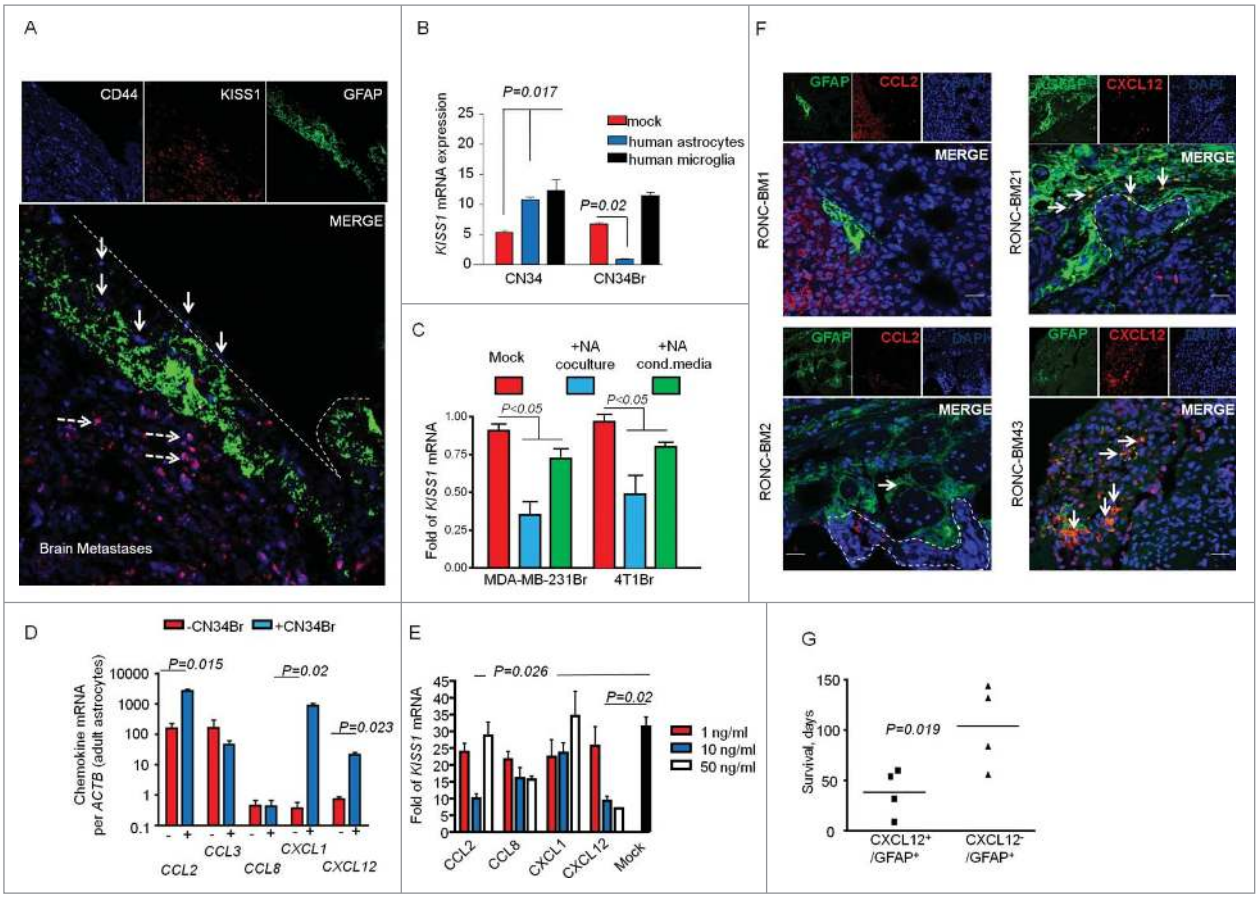

Figure 2. Normal astrocytes downregulate KISS1 in circulating BrCa cells via production of CXCL12/SDF1. (A) Immunofluorescence staining of brain metastatic specimen for KISS1 (red), stem cell marker CD44 (blue) and astrocyte marker GFAP (green), demonstrating that $CD44^+$ and $KISS1^+$ cancer stem cells (magenta colocalization signals) in the central part of the tumor (indicated by dashed arrows) loose expression of KISS1 ($CD44^+$ and $KISS1^-$ cells indicated by white solid arrows) upon contact with astrocytes that occurs at the tumor edge, i.e. the area of tumor invasion into the normal brain tissue. The white dashed line represents the physical edge of the tissue specimen; image magnification is 400X, scale bar: 20 μm. (B) Quantitative PCR analysis of *KISS1* mRNA expression in GFP-labeled CN34 or brain metastatic CN34Br BrCa cells with or without coculturing with either human astrocytes or human microglia cells (1:1 ratio). Expression of *KISS1* mRNA was determined in FACS-sorted GFP-positive cells. Total RNA was isolated as described in Materials and Methods, converted to cDNA and *KISS1* mRNA expression was quantified by RT-qPCR using the $\Delta\Delta$Ct method. Results were plotted after normalization to *ACTB* and presented as *KISS1* mRNA expression. Experiment was performed twice in triplicate. Red bars, *KISS1* mRNA in mock-treated control cells; blue bars, *KISS1* mRNA in cancer cells cocultured with human astrocytes; black bars, *KISS1* mRNA expression in the presence of human microglia; *P* values were determined using a Student *t* test; $P < 0.05$ indicates a significant difference in *KISS1* mRNA expression relative to mock-treated control cells. (C) RT-qPCR analysis of *KISS1* mRNA expression in GFP-labeled MDA-MB-231Br or 4T1Br metastatic BrCa cells after their coculturing with normal astrocytes (human or mouse, normal astrocytes (NA) coculture) or culturing in the presence of astrocyte conditioned medium (NA cond. medium) plotted as a bar graph. The experiment reveals downregulation of KISS1 expression upon contact with astrocytes or astrocyte-conditioned medium. Red bars, expression in mock treated cells; blue bars, expression following coculturing with astrocytes; green bars, expression resulting from incubation in astrocyte-conditioned medium. Experiment was performed twice in triplicate; $^*P < 0.05$ relative to mock-treated cells determined by the Student *t* test indicates statistical significance. (D) GFP-negative population of astrocytes cocultured with CN34Br cells were isolated by flow cytometry and total RNA was analyzed by real-time PCR to determine expression of various chemokines. Quantitative PCR for relative expression of the most regulated human chemokines *CCL2, CCL3, CCL8, CXCL12* and *CXCL1* was performed using cDNA from astrocytes cultured with (blue bars) or without (mock/red bars) CN34Br metastatic BrCa cells and presented as chemokine mRNA expression per housekeeping β-actin/*ACTB* mRNA (normalization control). Experiment was performed twice with 5 replicates per sample; $P < 0.05$ indicates statistical significance of changes assessed by a Student *t* test. (E) Treatment of CN34Br metastatic BrCa cells with recombinant CCL2 or CXCL12 proteins decreases *KISS1* mRNA levels as revealed by RT-qPCR analysis. Expression of *KISS1* mRNA in the presence of 1 (red bars), 10 (blue bars) or 50 (white bars) ng/ml of human CCL2, CXCL12, CXCL1 or CCL8 chemokines was analyzed and presented as *KISS1* mRNA copy number per *ACTB*; $P < 0.05$ indicate statistically significant differences determined by a Student *t* test. (F) Immunofluorescent detection of CCL2 or CXCL12 expression in GFAP-positive astrocytes. Paraffin-embedded brain metastatic tissue specimens were stained with GFAP (green signal), CXCL12/SDF1 or CCL2 (red signal) antibodies as described in Materials and Methods. Cells were counter-stained with DAPI for nuclei (blue). White dashed lines delineate tumor boundaries. White arrows indicate $GFAP^+$ and $CXCL12^+$ cells (yellow and orange colocalization signals). Image magnification is 400X, scale bar: 20 μm. (G) Analysis of possible correlation between survival of patients with BrCa brain metastases and the presence of $GFAP^+$ and $CXCL12^+$ astrocytes (with metastasis-induced CXCL12 and SDF1-expression) in their brain tissue specimens. The presence of $CXCL12^+$- and $GFAP^+$-positive astrocytes in metastatic tumor specimens inversely correlates with patient survival. Data presented as survival mean $\pm$ SD for each patient plotted against the number of $GFAP^+$ and $CXCL12^+$ cells; *P* value was calculated (relative to $GFAP^+$ and $CXCL12^-$ patients) by a Student *t* test with Welch correction; $P = 0.019$.

GFP-*KISS1*–3′UTR (Fig. 3C,D,F,G and S3) reporter construct (at 1 ng/ml) in CN34Br cells. A similar inhibitory effect was observed upon treatment of CN34Br cells with astrocyte-conditioned media ($P = 0.038$), which could be reversed by addition of AMD3100 ($P = 0.007$ relative to NHA-conditioned media treatment), a chemical inhibitor of CXCR4 signaling (Fig. 3E, H), strongly supporting involvement of CXCR4 in the mechanism of KISS1 downregulation. Conversely, transfection of MDA-MB-231Br cells with *MIR345–5p* mimic inhibited expression of *KISS1* mRNA (Fig. 4A, $P = 0.038$) or Luc-*KISS1*–3′UTR (Fig. 4B) reporter fusions by 50 to 60% relative to untargeted ("nontargeting") control miRNA ($P = 0.016$). On the contrary, no change in Luc expression was observed for a MUT 3′UTR construct bearing a mutation in the *MIR345* binding side within the *KISS1* mRNA 3′UTR sequence (Fig. S4). Finally, our data suggest that the expression of *MIR345* in tumors

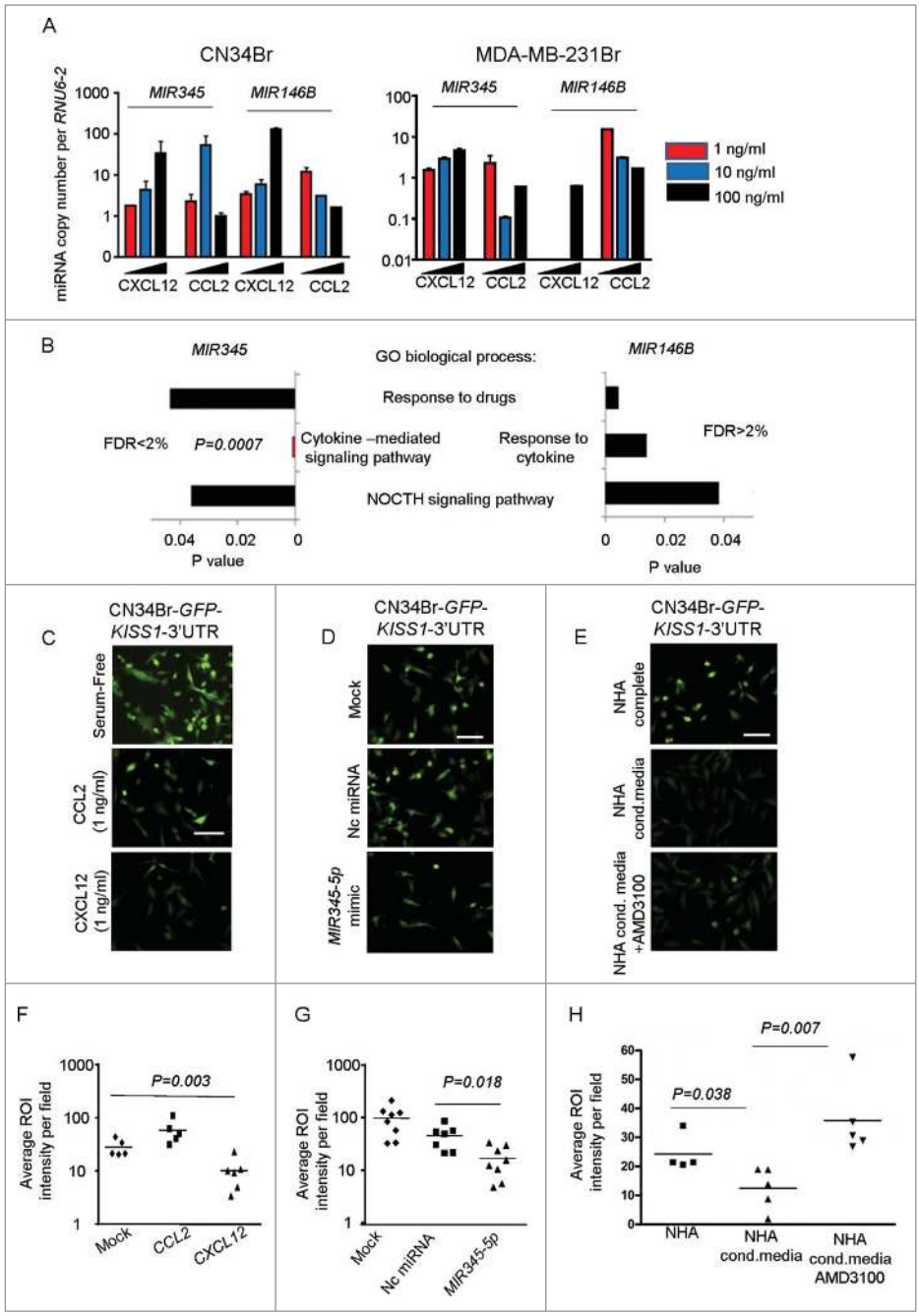

Figure 3. Downregulation of KISS1 by astrocyte-produced cytokines CXCL12 and CCL2 is mediated by a cellular *MIR345*. (A) A dose-dependent effect of CCL2 and CXCL12 cytokines on the expression of *MIR345* and *MIR146B* in CN34Br or MDA-MB-231Br BrCa brain metastatic cells 6 h after treatment of the cells with: 1 ng/ml (red bar), 10 ng/ml (blue bar) and 100 ng/ml (black bar) of either cytokine as determined by RT-qPCR. The data are presented as each miRNA copy number per *RNU6–2* (RNA, U6 small nuclear). Data represent results of 2 independent experiments, each performed in triplicates. (B) GO analysis of signaling pathways affected by cellular *MIR345* or *MIR146B*. The signaling pathway annotations were made based on scoring and evaluation of the pathways selected from the KEGG database (http://www.genome.jp/kegg). Although 22 pathways (GO term) with various *P* values were found to be regulated by *MIR345* or *MIR146B*, only statistically-enriched pathways ($P < 0.05$) are shown for simplification. For a complete list of pathways and analysis details please refer to Fig. S11. ((**C)and F**) Downregulation of KISS1 expression by CCL2 and CXCL12 proteins (at 1 ng/ml each) via a miRNA-mediated *KISS1* mRNA silencing as revealed by immunofluorescent analysis of CN34Br metastatic BrCa cells stably expressing a *GFP-KISS1*—3′UTR fusion reporter. The data summarize the results of 2 independent experiments, each performed in duplicates. Image magnification is 200X, scale bar: 50 μm (C). Quantitative analysis of GFP expression was performed using fluorescent images acquired by using a Nikon camera and ImageJ software; signal intensity from the region of interest (ROI) was quantified using an ROI manager. Data presented as an average ROI for each fluorescence image and sample; closed diamonds, mock-treated control cells; squares, CCL2-treated cells; closed triangles, CXCL12-treated cells; *P* values for changes vs mock-treated cells were calculated using the Student *t* test (F). (D and G) Puromycin-resistant CN34Br cells stably expressing a *GFP-KISS1*—3′UTR fusion reporter were transfected with the miRIDIAN precursor of human "mimic miRNA" *MIR345–5p* or a non-targeting miRNA as a negative control using a DharmaFECT1 transfection reagent; Nontransfected control cells were used as a (mock) control. Image magnification is 200X; scale bar: 50 μm (D). Quantitative analysis of GFP reporter expression was performed using fluorescent images collected 48 h post transfection, and analyzed (8 images per sample) by ImageJ after subtracting the background; other details as in (C). Closed diamonds, mock-treated cells; closed squares, nontargeting miRNA (Nc miRNA); closed triangles, *MIR345–5p*; *P* value of 0.018 relates to differences versus cells treated with nontargeting miRNA calculated using the Student *t* test (G). ((E)and H) Treatment of puromycin-resistant CB34Br cells stably expressing a *GFP-KISS1* 3′UTR fusion reporter with conditioned media from normal human astrocytes (NHA) demonstrates silencing of GFP expression in vitro. However, this silencing effect is attenuated in the presence of the CXCR4 inhibitor AMD3100. Images of BrCa cells were acquired after 48 h of incubation in the presence of astrocyte conditioned media ± AMD3100; image magnification is 200X, scale bar is 50 μm (E); Quantification details are as in G; closed squares-mock treated CB34Br cells; closed triangles-cells treated with NHA conditioned media; closed inverted triangles-cells pretreated with AMD3100 and incubated with NHA-conditioned media (H).

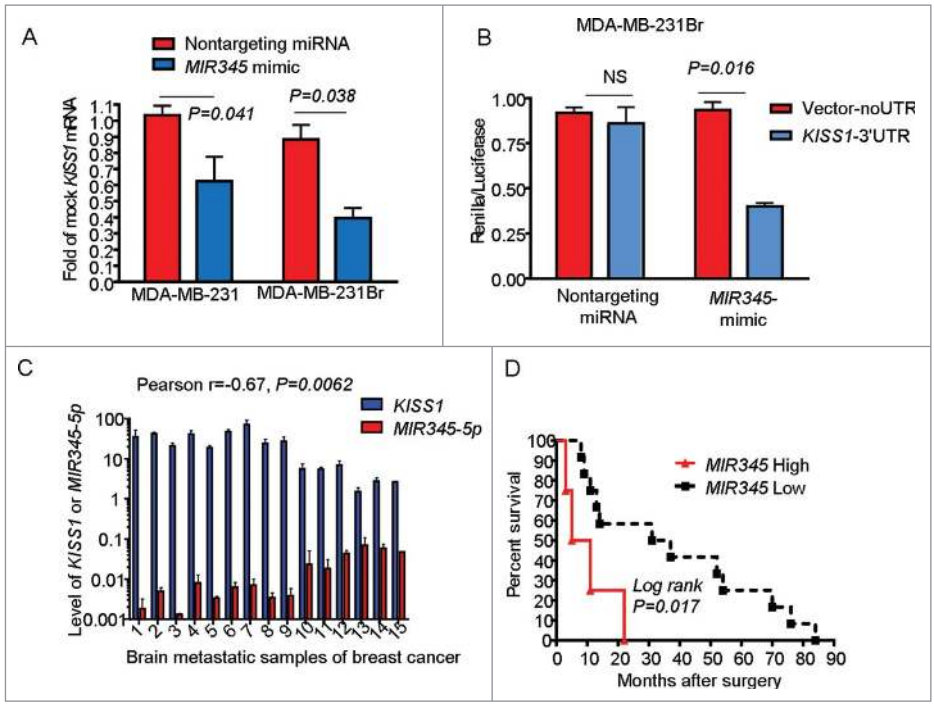

Figure 4. MIR-345–5p expression opposes KISS1 in breast cancer cells and primary samples. (A) Relative expression of *KISS1* mRNA following transfection of MDA-MB-231 or MDA-MB-231Br cells with either nontargeting miRNA (red bars) or *MIR345* mimic (blue bars) precursors as determined by RT-qPCR. (B) Relative expression of a Luciferase gene reporter with (blue bars) or without (red bars) the h*KISS1*—3′UTR sequence genetically fused downstream of the reporter-coding sequence in MDA-MB-231Br cells upon their cotransfection with *MIR345* mimic or nontargeting control miRNA. The h*KISS1*—3′UTR reporter fusion was under control of *CMV* promoter. Luciferase activity of samples was normalized to that of negative control and data presented as a relative fold difference ± SD. Data represent means of 2 independent experiments performed in triplicate; $P < 0.05$ indicates statistical significance determined by a Student *t* test. (C) Inverse correlation between expression of *MIR345–5p* and *KISS1* mRNA levels in human brain metastatic specimens as determined by RT-qPCR and the Pearson correlation test; Pearson coefficient $r = -0.67$, $P = 0.0062$; blue bars, *KISS1* mRNA copy number; red bars, human *MIR345* copy number both normalized by *ACTB* and *RNU6–2* housekeeping RNA. (D) A Kaplan-Meier survival curve for brain metastatic patients expressing either high or low levels of *MIR345–5p (MIR345*) as determined by RT-qPCR in the paraffin-embedded tissue samples. Statistical analysis is performed by a Log Rank Test, $P = 0.017$.

inversely correlates with the *KISS1* mRNA levels, whereas low expression of this miRNA is associated with longer survival of the patients with brain metastases (Fig. 4C,D). Altogether, our findings suggest that in CSC downregulation of *KISS1* expression occurs on a post-transcriptional (mRNA) level through expression of cellular *MIR345* modulated by the NHA-released chemokine CXCL12.

KISS1 inhibition promotes autophagy

Although BrCa cells can easily migrate to the brain, their survival in the brain tissue environment becomes a serious challenge. Because BCL2 expression is known[31,32] to be associated with cell survival and promoted by autophagy as well as antiapoptotic mechanisms, and since our data presented in Fig. 1 suggest a correlation between survival of tumor stem cells and their KISS1 deficiency, we stained primary specimens with BCL2- and KISS1-specific antibodies. We found a large population of brain-localized metastatic BrCa cells with upregulated BCL2, a marker of apoptotic resistance and autophagy survival (Fig. 5A,B), that were deficient in KISS1 expression. This finding suggests that KISS1 could be involved in the mechanism of cancer cell survival in the brain. To find out if KISS1 expression prevents metastatic cell survival in the brain, we ectopically overexpressed KISS1 in metastatic BrCa cells (Fig. S5). We observed that overexpression of KISS1 reduces ATG5 and ATG7 and inhibits conversion of LC3-I to LC3-II (Fig. 5C,D), which links KISS1 overexpression to autophagy inhibition. On the contrary, downregulation of KISS1 with the *KISS1*-KD61 shRNA construct reduces cellular accumulation of SQSTM1/p62 (1.47-fold). It has been shown that inhibition of SQSTM1 causes autophagic cell death in several human carcinoma cells.[33] Our data suggests that SQSTM1 downregulation is accompanied by upregulation of ATG5 (1.5-fold), ATG7 (1.4-fold) and conversion of LC3-I to LC3-II (autophagy markers), (Fig. 5E to H) in brain metastatic cells. This observation suggests that KISS1 expression can directly modulate autophagy. Besides, siRNA-mediated silencing of *Kiss1* improved the survival of 4T1Br BrCa cells (Fig. S6A) by suppressing apoptosis (Fig. S6C). In addition, KISS1 overexpression increased apoptosis (Fig. S6D). Furthermore, KISS1 knockdown resulted in the upregulation of *BECN1*/Beclin 1 mRNA (Fig. S7) and downregulation of SQSTM1 (Fig. 6A,B). Consistently with our observations, ectopic expression of KISS1 reduced ATG5 and ATG7 expression, while increasing accumulation of SQSTM1 (Fig. 6A). On the other hand, 3-methyladenine (3-Ma) inhibitor significantly suppressed autophagy in *KISS1*-KD61 (4-fold vs DMSO-treated) and control scrambled shRNA (1.6-fold vs DMSO-treated) MDA-MB-231Br-based cells, while pretreatment with bafilomycin A_1 (BafA1, an inhibitor of autophagosome maturation) promoted autophagy (~2.2-fold) as revealed by the increase in SQSTM1 expression in *KISS1*-KD61 cells vs shScrambled control cells (Fig. 6B). Finally, expression of KISS1 from an adenoviral vector in MDA-MB-231Br cells

exerted a synergistic effect with 3-Ma treatment by suppressing autophagy and promoting SQSTM1 expression (4.92-fold). Conversely, an ectopic expression of KISS1 (Fig. 6C) suppressed autophagy in MDA-MB-231Br cells, upregulated SQSTM1 (2.5-fold) and exhibited low level of LC3-II (1.75- vs 1.38-fold) in the presence of BafA1 in Ad-infected cells (empty vector control). Such correlation between KISS1 and SQSTM1 expression on both mRNA (Fig. 6E, $P = 0.015$) and protein

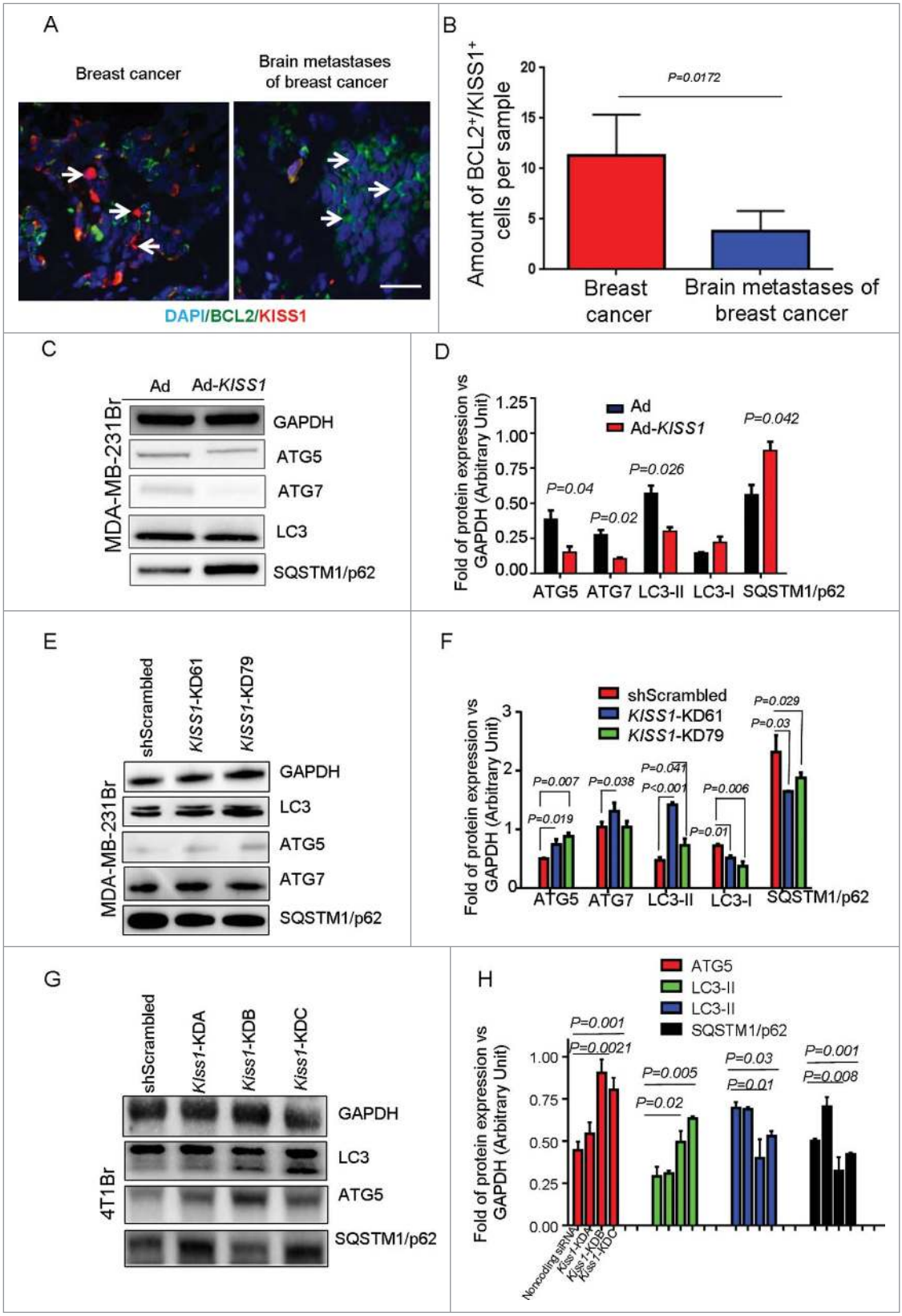

Figure 5. (For figure legend, see page 1912.)

(Fig. 6D,F) levels was also observed in human brain metastatic specimens (immunohistochemical [IHC] staining, Fig. 6D) and intracranial metastases of MDA-MB-231Br cells (yellow immunofluorescence signal (Fig. 6F), using intracranial route of tumor cells implantation, suggesting that downregulation of KISS1 in metastatic BrCa lesions in the brain leads to activation of autophagy.

Since coculturing of BrCa cells with NHA activates autophagy via KISS1 downregulation in BrCa cells, we sought to determine if this activation could improve anticancer properties of autophagy-dependent drugs such as temozolomide (TMZ) used to improve the efficacy of radiation therapy. Of note, combination of those approaches requires induction of autophagy.[34] In line with this suggestion, activation of autophagy via *KISS1* silencing increased antiproliferative activity of TMZ (20% to 65% depending on TMZ concentration) (Fig. 7A,B). Furthermore, prior treatment of *KISS1*-KD79 knockdown MDA-MB-231Br cells with an autophagy inhibitor 3-Ma, reduced TMZ-associated cytotoxicity 2-fold ($P < 0.05$) (Fig. 7C,D). These findings underline the important role of KISS1 in the mechanism of metastatic brain tumor sensitivity to cytotoxic agents and suggest high therapeutic potential of autophagy-modulating agents for the treatment of brain metastases.

Downregulation of KISS1 in BrCa cells promotes their metastatic invasiveness into the brain

To understand the role of KISS1 protein in the fate of BrCa cells disseminated in the brain we assessed the metastatic potential of KISS1-deficient cells. Since astrocytes can produce mediators of metastases, we hypothesized that expression of CXCL12 could induce metastatic activity in CN34Br and MDA-MB-231Br cells. Previously KISS1 was reported to suppress invasion and migration of both normal[6,35] and cancerous[36,37] cells. Interestingly, KISS1 expression has previously been reported to inversely correlate with that of MMP9,[38,39] known to promote invasion[40,41] and migration[42] of BrCa cells. As shown in Fig. 8A to D, KISS1-deficient cell lines *KISS1*-KD61, *KISS1*-KD79 (MDA231Br-based) and *Kiss1*-KDA (4T1Br-based) exhibit a 2- to 3-fold increased migration toward media enriched with SDF-1a chemokine and 2- to 100-fold increase in invasiveness (Fig. S8). Whereas inhibition of autophagy, using RNA interference against human *ATG5* (Fig. 8E,F and Fig. S9), decreased invasiveness from 163.8 ± 13.8 to 47.4 ± 11.4 cells (BrCa 71% reduction, $P < 0.0001$), ectopic expression of KISS1 (Fig. 8G,H) in KISS1-deficient cells repressed autophagy-mediated invasion from 65.4 ± 9.21 to 47.6 ± 13.1 (~27% reduction, $P = 0.017$) cells. Additionally, knockdown of *KISS1* mRNA by shRNA silencing induced expression of MMP9, which inversely correlated with that of KISS1 in patient tumor specimens[43] as revealed by their IHC staining (the Fisher exact test, $P < 0.001$) (Fig. 9A). This was consistent with our earlier findings that MMP9 expression directly correlates with metastatic progression of BrCa.

Recently, Cheng et al., and earlier Milovanovic et al., have found a direct correlation between MMP9 and IL8 expression levels and tumor progression in nasopharyngeal carcinoma[44] and BrCa patients,[45] respectively. Since expression of MMP9 inversely correlates with expression of KISS1 and directly with that of IL8,[46] we reasoned that expression of KISS1 could negatively affect IL8 expression. Indeed our antibody array data presented in Fig. S10 demonstrates that downregulation of KISS1 is associated with upregulation of IL8, which, in turn, could contribute to tumor invasion and metastatic progression. Furthermore, immunofluorescence analysis of brain tumor specimens (Fig. 9B) confirms our in vitro finding that KISS1-specific staining does not colocalize with that for IL8, whose induction is linked to cancer metastatic progression possibly via yet another mechanism.

Discussion

Although normal adult astrocytes are critical for maintaining brain homeostasis, recent data suggest that they also play an important role in establishing brain metastases in patients with advanced form of BrCa.[14] The results of our study suggest a new mechanism for the early stage of BrCa metastases in the brain that involves a tumor suppressor factor termed KiSS-1 metastasis-suppressor (KISS1). According to the proposed mechanism, regulation of KISS1 expression, critical for realization of metastatic potential of circulating BrCa cells entering the brain, occurs on post-transcriptional level and involves cellular *MIR345*. The latter is induced in BrCa cells in response to chemokine CXCL12 produced in the brain environment by normal adult astrocytes. Our study provides the first evidence that a population of circulating BrCa stem cells crossing the blood brain barrier and entering the brain induces and activates expression of chemokines in NHA, which in turn mediate

Figure 5. (see previous page) KISS1 regulates autophagy in the brain metastatic cells. (A) Immunofluorescence staining of paraffin-embedded sections of BrCa and brain metastatic BrCa tissues using anti-KISS1 (red, cytoplasmic and nuclear staining), anti-BCL2 (green, cytoplasmic staining) fluorescently-labeled antibodies and DAPI (blue, DNA staining) to visualize nuclei. Numerous cells with robust KISS1 expression identified by bright red signal (white arrows) or yellow and orange signal (in cells with visible colocalization of KISS1 and BCL2 signals), are present in representative tissue specimens. In contrast, brain metastatic BrCa tissue contains almost no KISS1-positive cells, but large number of cells expressing BCL2 suggesting a correlation between downregulation of KISS1 in metastatic cells and their resistance to apoptosis. Image magnification is 400X, scale bar: 20 μm. (B) Relative expression of $BCL2^{+}$- and $KISS1^{+}$-positive cells detected in 4 BrCa tissue specimens and 4 brain metastatic lesions of BrCa. The data are presented as amount of BCL2- and KISS1-positive cells detected in the patient samples ± SD. All changes are statistically significant ($P = 0.0172$ calculated by the Student *t* test). (**C, D**) Expression of human KISS1 in Ad-*KISS1* vector-transduced MDA-MB-231Br cells results in suppression of autophagy. The cells (2×10^5) were infected with Ad or Ad-*KISS1* vectors at a multiplicity of infection of 1 and the levels of autophagy-related proteins SQSTM1, LC3-II, ATG5 and ATG7 were analyzed by western blot (C), followed by densitometry-based semi-quantification, which is presented as a relative protein expression normalized by GAPDH as a loading control (D); black bars, control adenovirus (Ad)-infected cells; red bars, cells infected with human *KISS1*-encoding adenovirus (Ad-*KISS1*). The experiment was performed 3 times and average data are presented. (E to H) Knockdown of *KISS1* by shRNA-mediated silencing induces autophagy in MDA-MB-231Br and 4T1Br cells. The cells were transduced with lentiviral vector or siRNA duplexes to generate stable or transient cell lines with silenced *KISS1*/*Kiss1* expression. Stable cell lines with silenced *KISS1* expression (*KISS1*-KD61 and *KISS1*-KD79), based on MDA-MB-231Br (E, (F)top panels), or transient 4T1Br-based cell lines *Kiss1*-KDA, *Kiss1*-KDB and *Kiss1*-KDC with siRNA-silenced *Kiss1* expression (G, H), were used to analyze the autophagy response by assessing expression levels of ATG5, ATG7, SQSTM1 as well as LC3 form I to form II conversion rate by western blot (E, G). Cells expressing shScrambled or noncoding siRNA were used as a nontargeting control. The relative protein expression was quantified by semi-quantitative densitometry (F, H). The experiment was performed 3 times and representative data are shown.

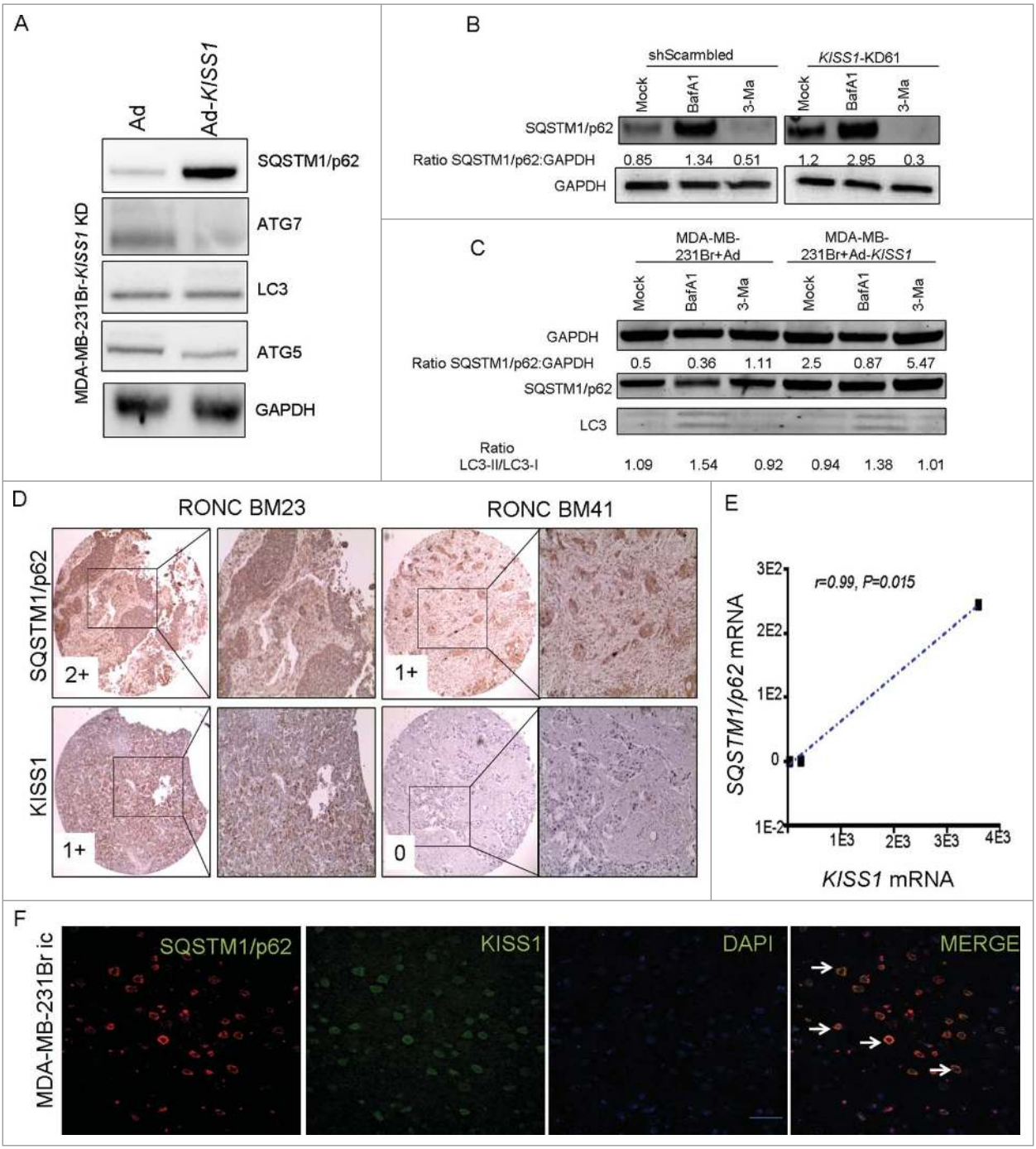

Figure 6. KISS1 expression correalates with p62/SQSTM1. (A) KISS1 expression reverses autophagy induction in the model of MDA-MB-231Br cells lacking KISS1 expression (MDA-MB-231Br-*KISS1*KD). Western blotting assessment of ATG7, LC3, ATG5, SQSTM1 and human GAPDH during KISS1 infection by selfreplicating oncolytic adenovirus. Experiment was conducted twice and data from one experiment are shown. (B and C) KISS1 knockdown promotes autophagy in MDA-MB-231Br cells. (B) Lentivirus-transduced MDA-MB-231Br cell lines shScrambled or *KISS*-KD61 were pretreated with DMSO, 1 mM of 3-Ma or 1 nM of BafA1 for 4 h and cell lysates were prepared and analyzed by western blots 48 h later using 10 μg of total protein loaded on each lane and the membrane was incubated with SQSTM1- or GAPDH-specific antibodies. (C) Ad or Ad-KISS1-transduced MDA-MB-231Br cells were pretreated with DMSO, 1 mM of 3-Ma or 1 nM of BafA1 for 4 h and cell lysates were prepared and analyzed by western blots 48 h later using 10 μg of total protein loaded on each lane and the membrane was incubated with SQSTM1- or GAPDH-specific antibodies. (D to F) Representative IHC or immunofluorescence images of brain metastatic BrCa (RONC-BM41 and RONC-BM23) human tissue specimens (D, E) or mouse-implanted MDA-MB-231Br human intracranial xenografts (F) stained for SQSTM1 and KISS1 demonstrate a direct correlation between *KISS1* and *SQSTM1* gene expression. IHC staining intensity for KISS1 (graded as 0 and 1+) showed direct correlation with that for SQSTM1 (graded as 1+ and 2+) in RONC-BM41 and RONC-BM23, respectively (D). Original image magnifications are 200X (scale bar: 50 μm) and 400X (scale bar: 20 μm); expression of SQSTM1 and KISS1 was visualized using brown dye DAB, conjugated to secondary antibody with background staining with blue dye haematoxylin or using an avidin-biotin conjugation system (F). A direct correlation between expression of *SQSTM1* and *KISS1* was also validated by RT-qPCR analysis of the corresponding gene's mRNA expression (E) as well as IF staining of murine intracranial MDA-MB-231Br xenografts (MDA231Br ic, (F) counterstained with DAPI using human KISS1- and SQSTM1-specific antibodies. White arrows indicate BrCa cells with detectable KISS1 (red signal) expression that in most cells colocalizes with SQSTM1 (green signal) producing orange foci (white arrows) on the merged (400X) image; scale bar: 20 μm. Spearman correlation test between *KISS1* and *SQSTM1* mRNA expression was used to analyze the mRNA expression results (E) ($r = 0.99$, $P = 0.015$).

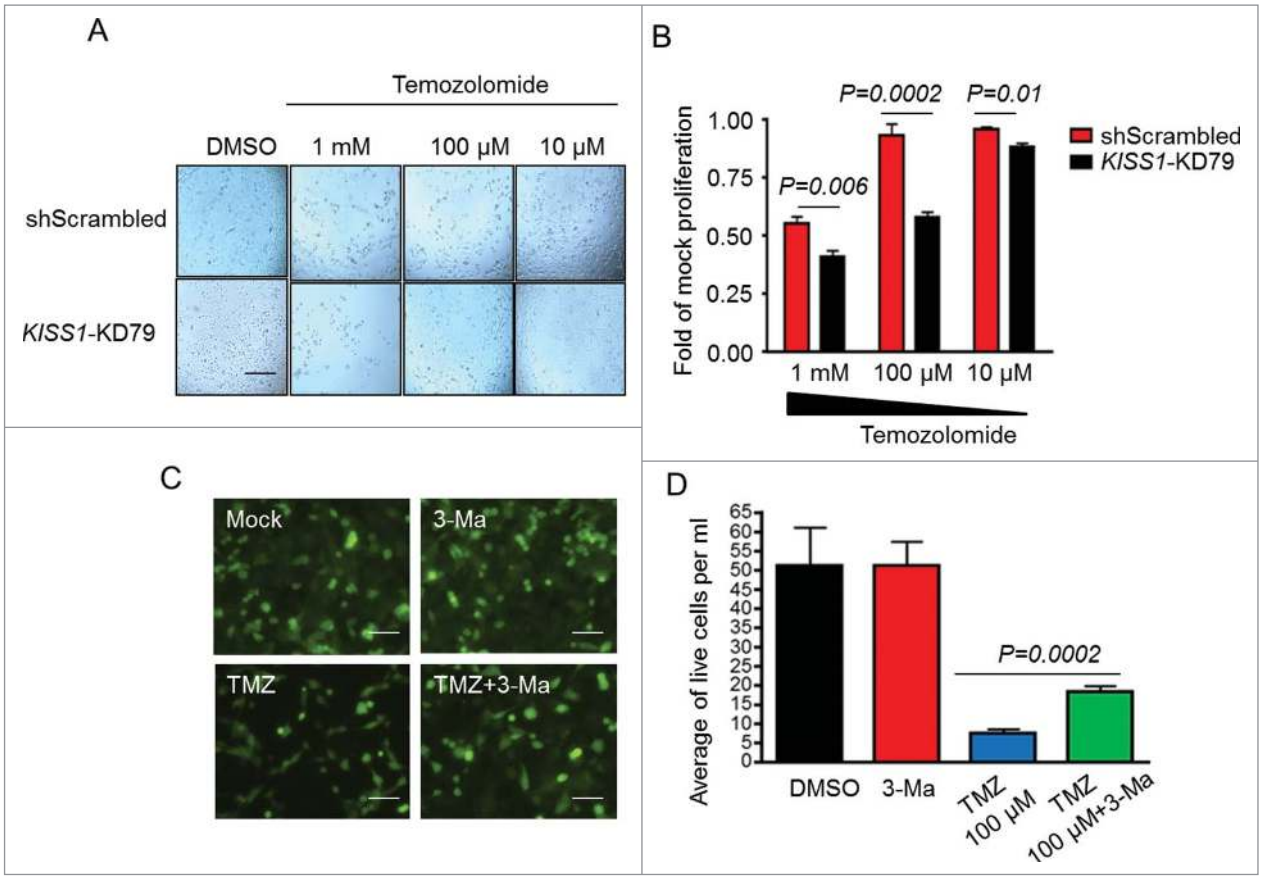

Figure 7. Downregulation of KISS1 improves sensitivity of BrCa cells to temozolomide (TMZ). To observe KISS1-mediated sensitization of TMZ-resistant MDA-MB-231Br cells a total of 4×10^3 cells, stably expressing either a nontargeting (shScrambled control) or a *KISS1*-targeting (*KISS1*-KD79) shRNAs, were treated with increasing doses of TMZ (10 μM, 100 μM and 1 mM) for 72 h. Cell viability was assessed by light microscopy. (A) Phase-contrast images were collected under a 100X magnification; scale bar: 100 μm; Relative proliferation rates of the control and the KISS1 knockdown cells was determined by MTT assay (B); red bars, shScrambled cells; closed and black bars, *KISS1*-KD79 cells. The data are presented as fold (mean $\pm$ SD) of mock proliferation; statistical significance of the changes ($P < 0.05$) vs control cells (shScrambled) was determined using the Student *t* test. (C) The effect of autophagy inhibitor 3-Ma on sensitivity of BrCa cells with KISS1 knockdown to temozolomide (TMZ) in vitro. GFP-labeled *KISS1*-KD79 cells were pretreated with DMSO alone (mock) or 1 mM DMSO solution of 3-Ma for 2 h before 96 hr treatment with 100 μM TMZ. Images were collected at selected time point using a Nikon Ti-U eclipse microscope under a 200X magnification; scale bar: 50 μm; green fluorescence, GFP-labeled cancer cells. (D) Quantification of live cells after treatment with TMZ in the presence or absence of autophagy inhibitor 3-Ma (described in C) by trypan blue exclusion test; closed and black bars, DMSO only/no treatment control; red bars, treatment with 3-Ma in DMSO; blue bar, treatment with 100 μM TMZ alone; green bar, treatment with 100 μM TMZ+3-Ma. Experiment was performed twice in triplicate. Statistical significance of the change relative to the TMZ only-treated group ($P = 0.0002$) was determined by the Student *t* test.

downregulation of KISS1 expression in those BrCa cancer stem cells following their localization to the brain. A direct interaction with the astrocytes promotes invasion of the cancer cells into the brain parenchyma. We showed that a 24-h incubation of astrocytes (NHA) in the presence of BrCa cells is sufficient for the induction and release of CXCL12 and CCL2 by those astrocytes. The results of our experiments are consistent with high levels of CCL2[47] and CXCL12 expression found in patients with advanced stage (metastatic) BrCa.[48] We cannot rule out the possibility of autocrine regulation of CCL2 or CXCL12 (splicing variants such as CXCL12α, CXCL12β or CXCL12γ) expression in astrocytes, especially given the fact that CXCL12α serves as chemoattractant for the recruitment of immune cells, such as T cells and monocytes.[49,50] Although, expression of chemokines, such as CCL2 and CXCL12, in normal brain is low, it can be stimulated in astrocytes by various factors.[51] Our hypothesis is that astrocytes together with monocytes can contribute to brain metastases by secreting CCL2 and CXCL12. A most recent study by Lee et al. suggests that inhibition of CXCR4-CXCL12 signaling suppresses migration of circulating cancer cells through brain endothelium.[52]

The astrocyte-CN34Br model is unique in that it recapitulates interaction between astrocytes and cancer cells critical for the onset of brain metastatic disease. Our data also suggest that the release of CCL2 and CXCL12 by astrocytes facilitates the survival of the cancer cells in the brain. It is, however, not clear how secretion of CCL2 and CXCL12 by astrocytes can also contribute to inflammation as one of the hallmarks of cancer progression. The latter cannot be ruled out because expression of inflammatory chemokines is known to promote metastases. Sensitivity of astrocytes to various stresses is consistent with the induction of chemokines, such as CCL2, by chemotherapeutics.[53,54]

Our study suggests that downregulation of tumor suppressor KISS1 could activate expression of proinvasive factors MMP9 and IL8. We did not aim to investigate the precise mechanism of MMP9 and/or IL8 upregulation, but our unpublished data suggest that *KISS1* silencing can activate expression of transcription factors TFAP2A/AP-2a, SP1/SP-1 and induce phosphorylation of inhibitory NFKBIA/IκBα protein, essential for activation of NFKB1/NF-κB. On this basis, we speculate that activation of downstream targets, such as IL8, can occur

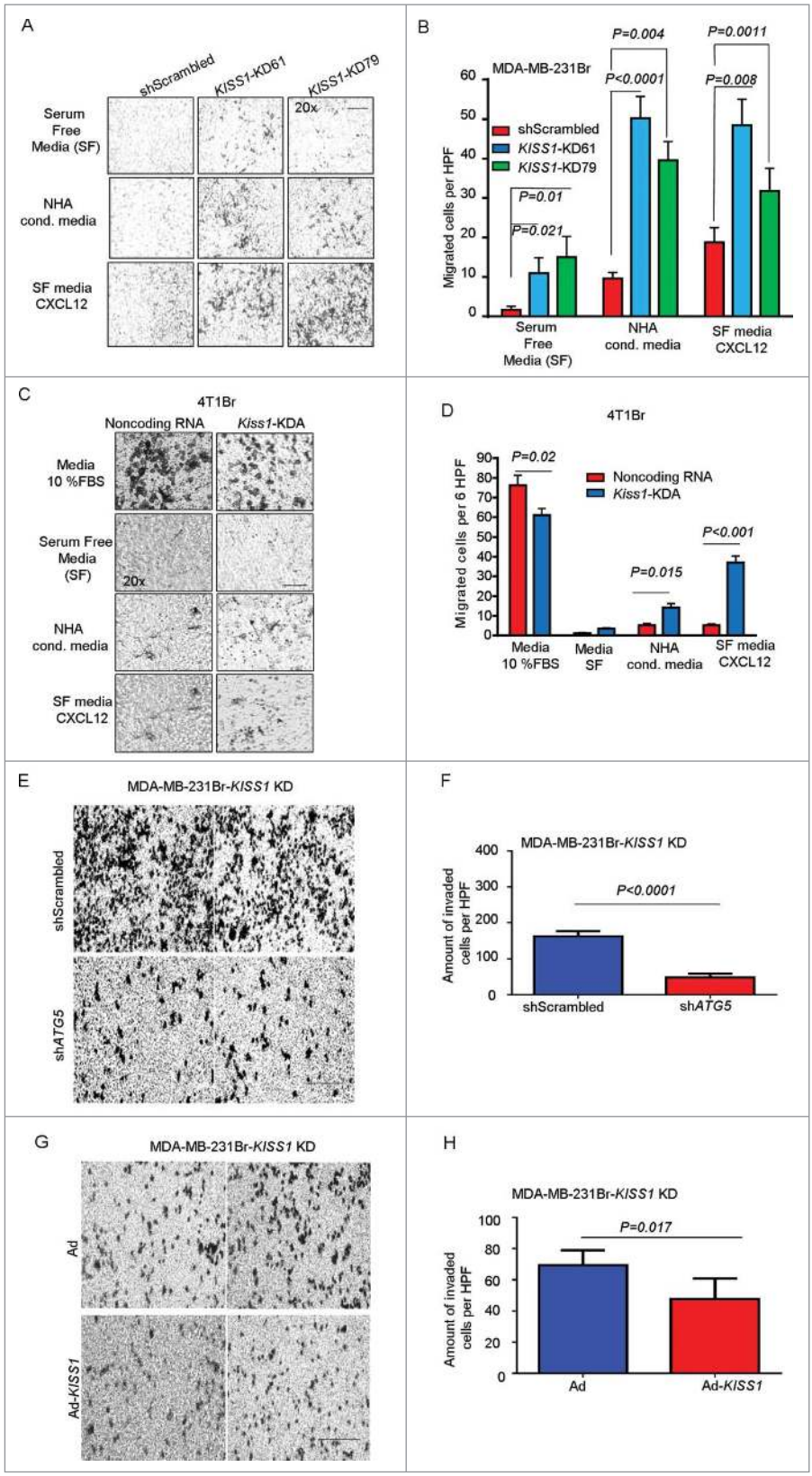

Figure 8. KISS1-mediated suppression of autophagy promotes cancer cell migration. (A,C, E and G) Transwell motility assays using shScrambled, *KISS1*-KD61, *KISS1*-KD79 cells (MDA-MB-231Br-based) (A), noncoding miRNA and *Kiss1*-KDA (mouse 4T1Br-based) (C), KISS1 stable knockdown MDA-MB-231Br cells transfected with shScrambled or sh*ATG5* (E) or preinfected with Ad or Ad-*KISS1* 48 h before loading on Matrigel-coated transwell plates, were performed on 8-μM inserts for 24 h in triplicates. DMEM supplemented with 10% FBS, serum-free medium, astrocyte-conditioned medium with or without CXCL12, as a chemoattractant, were added to the lower transwell chamber of each sample. The migrated cells were stained with 0.4% crystal violet and counted. Representative images of MDA-MB-231Br or 4T1Br-based cells were generated in triplicates from 2 independent experiments under magnification of 400X; scale bar: 20 μm. (B,D, F and H) Quantitative assessment of migrated cells shown in panels (A,C, E and G), respectively. A 2- to 4-fold increase in migration of *KISS1*-KD61 and *KISS1*-KD79 cells was observed in both MDA-MB-231Br-based (B) and 4T1Br-based (D) *KISS1* knockout cells. Bars represent the numbers (means $\pm$ SD) of migrated cells per high power field (HPF).

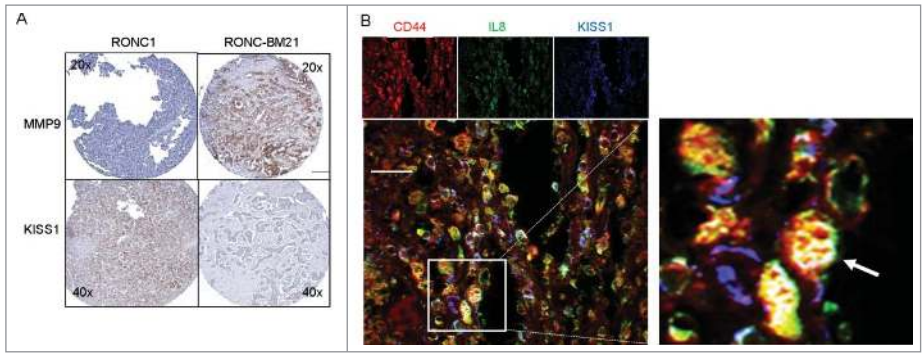

Figure 9. KISS1 expression inversely correlates with MMP9 and IL8. (A) Representative images of IHC staining of primary (IDC) and metastatic (RONC-BM21) tumor specimens with MMP9- and KISS1-specific antibodies; 5 μM-matched specimens obtained from the same patients show high expression levels of KISS1 (brown, cytoplasmic staining) and low levels of MMP9 (brown, membrane and cytoplasmic staining) in the primary BrCa (IDC), but high MMP9 and low KISS1 levels in brain metastases (RONC-BM21); image magnifications are 200X; scale bar: 50 μm. (B) IF staining of primary metastatic specimen for IL8, CD44 and KISS1 markers. Representative IF staining for IL8 (pseudocolored with green), KISS1 (pseudocolored with blue), CD44 (pseudocolored with red) is shown with image magnification of 400X; scale bar: 20 μm; White arrow shows colocalization of IL8 and CD44 in some IL8$^+$, CD44$^+$ and KISS1$^-$ brain metastatic cells (yellow signal, solid arrow). Inset (right image panel) shows a blow-up image (600X) of the squared area of the tri-color merged 400X image (scale bar: 20 μm).

via binding of transcription factors to the correspondent promoters and/or binding of the NFKB1/NF-κB-RELA/p50-p65 heterodimer complex to the promoter elements of downstream genes. The results of our study also suggest that induction of chemokines by astrocytes leads to upregulation of cellular microRNAs capable of modulating metastatic potential of cancer cells via downregulating KISS1 expression. We discovered that *MIR345* and *MIR146B* are important effectors of cancer cell metastatic transformation since they can regulate KISS1. Besides KISS1, *MIR345* and *MIR146B* regulate as many as 400 different targets involved in angiogenesis, cell adhesion etc., some of which also prevent metastatic progression of cancers. Therefore, future data mining analyses will be performed to examine the mechanism regulating expression of *MIR345* and its other potential targets as well as their possible relationship. Interestingly, our findings are consistent with recent data suggesting that CXCL12 activates expression of prometastatic microRNAs.[29] Our data suggest that CXCL12 and CCL2 are important effectors of metastatic development of BrCa.

Because cancer cell survival is one of the key conditions for the development of metastases, we addressed the importance of KISS1 expression for the survival of metastatic cancer cells. We found that knockdown of KISS1 exerts a stimulating effect on expression of ATG5, implicated in autophagosome maturation. Although in our experiments *ATG5* gene silencing by an RNA interference mechanism was validated independently with 3 different *ATG5*-specific probes at both western blot and real-time qPCR levels and found to interfere specifically with autophagy-related cellular signaling, we cannot entirely rule out off-target effects mediated by siRNA partial complementarity to mRNAs of other genes.[55,56] In our experiments, we observed no changes in *GAPDH* or *ACTB* mRNA expression in the presence of siRNAs against human *ATG5* gene suggesting specificity of *ATG5* mRNA downregulation. Previously, using a hepatocellular carcinoma model, inhibition of autophagy was found to suppress tumor growth and improve cytotoxicity mediated by cisplatin.[57]

Taken together, our data demonstrate that adult astrocytes mediate suppression of KISS1 expression via the CXCL12-*MIR345* paracrine loop that can promote BrCa cell invasiveness and survival in the brain. We also show for the first time that KISS1 knockdown affects downstream targets determining cancer cell survival and resistance to chemotherapy. Further studies are needed to identify therapeutic strategies for targeting KISS1-negative population of metastatic cancer cells in the brain, which could potentially improve survival of patients with advanced BrCa disease.

Materials and methods

Cells

Metastatic BrCa clones "brain seeking clones" of CN34Brm2Ctgl (CN34Br), GFP and nonlabeled MDA-MB-231Br, and parental cells CN34TGL (CN34) were obtained from Dr. Patricia Steeg (Center for Cancer Research, NIH, Bethesda, MD) and Dr. Joan Massague (Sloan-Kettering Institute, NY) in compliance with the institutional material transfer agreements. MDA-MB-231 cells were originally purchased from ATCC (HTB-26). BrCa tumor circulating cells MDA-MB-231Cherry and MDA-MB-231GFP (MDA231BrGFP) were obtained from Dr. Dmitry Malin (UW-Endocrinology) and Jennifer Koblinsky (VCU), respectively. The MDA-MB-231- and CN34-based cells were cultured in the media described elsewhere.[26,58] Briefly, MDA-MB-231Br cells were cultured in DMEM/F12 medium supplemented with 10% fetal bovine serum (FBS; Atlanta Biologicals, S11195H) and 100 U/ml penicillin/streptomycin; CN34 cells were cultured in M199 medium supplemented with 2.5% FBS, 10 μg/ml insulin (Sigma-Aldrich, I9278), 20 ng/ml EGF (Sigma-Aldrich, 324831), 100 ng/ml cholera toxin (Sigma-Aldrich, C8052), 0.5 μg/ml hydrocortisone (Fisher Scientific, NC9881403) and 100 U/ml penicillin/streptomycin.

Primary adult human (1800) and mouse (M1800) astrocytes and microglia (1907) were obtained from ScienCell and cultured in the media suggested by the vendor. Complete conditioned media was obtained by culturing of primary astrocytes in media from ScienCell for 6 d without change of media.

Human brain and BrCa specimens

The protocol for the use of primary specimens in the current study was approved by the Russian Oncology Center, Moscow, Russia IRB committee. A pilot tissue microarray from 10

Table 1. Characteristics of specimens used in this study.

Specimen /tissue type	Specimen name	Patient live status*	Age at IDC diagnosis	IDC grade	Brain Met year of diagnosis	TNM	ER	PR	HER-2
Brain Metast. Sample	RONC-BM	living	61	IIB	2000	T1N0M0	Neg	Neg	Neg
	RONC-BM1	living	67	III	2004	T2N1M0	Neg	Neg	Pos
	RONC-BM2	deceased	45	IIa	2005	T2N0M0	Neg	Neg	Neg
	RONC-BM21	living	75	II	2002	T2N0M0	Neg	Neg	Neg
	RONC-BM23	living	31	II	2005	T2N1M0	Neg	Neg	Pos
	RONC-BM31	living	59	III	2002	T2N1M0	Neg	Neg	Pos
	RONC-BM34	deceased	65	III	2005	T1N1M0	Neg	Neg	Pos
	RONC-BM37	deceased	57	IIIa	1996	T2N0M0	Neg	Neg	Pos
	RONC-BM39	deceased	70	IIIa	2005	T3N2M0	Neg	Neg	Neg
	RONC-BM41	living	35	III	2008	T2N1M0	Neg	Neg	Pos
	RONC-BM43	living	71	III	2006	T2N0M0	Pos	Pos	Pos
	RONC-BM47	deceased	68	III	2003	T2N0M0	Neg	Neg	Neg
	RONC-BM61	living	47	IIIa	1994	T2N2M0	Neg	Neg	Neg
	RONC-BM74	living	59	III	2004	T2N0M0	Pos	Pos	Pos
	RONC-BM321	deceased	50	IIB	2007	T2N1M0	Pos	Neg	Neg
Primary BrCa Sample	RONC1	living	79	III		T2N0Mx	Pos	Pos	Neg
	RONC2	living	66	III		T2N2Mx	Pos	Pos	Neg
	RONC4	living	40	II		T1N0Mx	Pos	Pos	Neg
	RONC10	living	75	III		T2N2aMx	Pos	Pos	Pos
Normal breast tissue	Normal1	living	45			T0N0M0			
	Normal2	living	40			T0N0M0			
	Normal3	living	37			T0N0M0			
	Normal4	living	39			T0N0M0			
	Normal5	living	33			T0N0M0			

Abbreviations: *Status as of 11/11/2015; BrCa – breast cancer; IDC grade – the grade of invasive ductal carcinoma (IDC) in patients when diagnosed with brain metastases; TNM-breast cancer staging based on tumor size, cancer spreading to lymph nodes and metastasis occurrence; ER, PR and HER2- status of estrogen, progesterone and HER2 receptors in tissue specimens detected by immunohistochemistry, respectively. Neg- negative status; Pos- positive status;

patients with brain metastatic disease, matched and unmatched primary BrCa specimens of BrCa and 5 control patients was created (Table 1). Primary BrCa tissue samples are: RONC1, RONC2, RONC4 and RONC10. The brain metastatic BrCa specimens are: RONC-BM, RONC-BM1, RONC-BM2, RONC-BM21, RONC-BM23, RONC-BM35, RONC-BM41, RONC-BM43, RONC-BM61 and RONC-BM321. Additionally, a tissue microarray containing BrCa from US Biomax (BR1008) was used for immunofluorescence and immunohistochemistry.

Mouse specimens

Mouse xenografts of human MDA-MB-231Br (MDA231Br) cells were obtained from an earlier study.[23]

Drugs and proteins

AMD3100 chemical inhibitor (A5602) and 3-Ma autophagy inhibitor (M9281) were purchased from Sigma-Aldrich, Bafilomycin A_1 (BafA1, 196000) was obtained from Calbiochem-EMD Millipore and temozolomide (T1849) was obtained from LKT.

Human recombinant CCL2 (MCP-1, 300–04), CCL8 (MCP-2, 300–15), CXCL1 (GRO-α/MGSA; 300–11), CXCL12 (SDF1α; AF-300–28A) proteins were purchased from Peprotech.

siRNA and shRNA constructs

shRNA plasmids targeting the human *ATG5* gene (Origene, TG314610; sh*ATG5* versions A, B, C and D) and "scrambled" negative control (nontargeting shRNA cassette in pGFP-V-RS vector plasmid TR30013, Origene) were transfected into MDA-MB-231Br using DharmaFECT1 transfection reagent (GE Dharmacon, T-2001–01). Selection of stably-transfected clones was performed using puromycin (Invivogen, ant-pr-1) selection at 6 μg/mL antibiotic concentration. A mixture of 3 siRNA duplexes against mouse *Atg5* (sc-41446) or *Kiss1* genes (versions *Kiss1*-KDA [SR402044A], *Kiss1*-KDB [SR402044B] and *Kiss1*-KDC [SR402044C]), and scrambled negative control siRNA duplex (SR30004), purchased from Santa Cruz Biotechnology and Origene, were transiently transfected into 4T1Br cells.

Viral vectors

Lentiviruses, expressing the 3′ UTR of the human *KISS1* gene, shRNAs against human *KISS1 (KISS1*-KD61 and *KISS1*-KD79), or scrambled control shRNA (shScrambled) were obtained from ABM Inc.).

Recombinant adenovirus construction. The genome of the conditionally replicative adenovirus with mCherry red fluorescent protein on the capsid was constructed by 2-step homologous recombination (HR) in *E. coli* (BJ5183 strain) using a described previously E3/fiber-modified Ad5 backbone vector Ad5Δ*E1*/Δ*E3*, F5/3[59] and a modified *E1* shuttle vector, pSlΔ24-pIX-mCherry. The E1 shuttle vector contained a fluorescent reporter mCherry coding sequence,[60] inserted downstream of the Ad5 minor capsid protein IX (pIX) gene via a linker sequence, encoding a 10-amino acid peptide (SADYKDDDDK) with an octapeptide flag motif (in bold). The flag was followed by NheI restriction site used for mCherry coding sequence (CDS) insertion to generate a pIX-Flag-mCherry fusion with expression controlled by the native pIX promoter. The shuttle also harbored a 24-base pair deletion in the Ad5 *E1A* gene coding sequence ("Δ24′), as described previously, to render Ad5

replication selective for cancers with disrupted retinoblastoma (Rb) tumor suppressor pathway.[61]

The intermediate backbone vector Ad5Δ*E1*/Δ*E3*, CMV-*KISS1*, F5/3 was generated by HR in bacteria between the fiber gene-modified vector Ad5Δ*E1*/Δ*E3*, F5/3[62] and an *E3* shuttle vector, harboring deletion of the E3 region sequence starting from the last 44 bases of the *E3A* 12.5K gene CDS up to the last 18 nucleotides of the *E3B* 14.7K CDS. The *KISS1* cassette was PCR amplified using sense and antisense primers and cloned into the unique SalI site of the above E3 shuttle downstream of the SwaI site-flanked kanamycin (*Kan*) gene. Following homologous recombination (HR) of the fiber-deleted backbone plasmid with the modified *E3* shuttle recombinant clones were screened using 2 sequential PCR-assays detecting Ad5 pIX (or Ad5 hexon) gene-specific sequences followed by detection of the 3′ knob sequences of the F5/3 fiber chimera. Since the E3 shuttle vector carried the wild-type fiber gene sequence as part of one of its "recombination arms" (RA), the latter assay was performed to verify that HR occurred upstream of the Ad3 knob domain sequence of the Ad5ΔE1/ΔE, KISS1, F5/3 backbone vector and the Ad3 knob sequence of the F5/3 chimera fiber gene was not replaced by the Ad5 knob sequence of the *E3* shuttle. Incorporation of the Kan gene in the intermediate backbone plasmid allowed selecting recombinants on 2 antibiotics: Amp and Kan. Following HR of the Ad5Δ*E1*/Δ*E3*, CMV-Kiss1, F5/3 with the PmeI-linearized *E1* shuttle vector pSlΔ24*E1*, pIX-mCherry and colony selection on Kan, the *E1* recombinants were screened using a PCR assay. The accuracy of HR was additionally verified by restriction digest with HindIII and NheI. A mixture of 2 nonrecombined plasmids was used as a control to account for a strand switch as a possible mechanism for false-positive signal. Miniprep plasmid DNA isolated from positive BJ clones was retransformed in the stable strains STBL4 or DH5-α (Invitrogen), and following colony rescreening and plasmid upscaling, linearized with PacI and transfected into the HEK-293 helper cells with Lipofectamine 2000 (Thermo Fisher-Invitrogen, 11668027).

Generation and molecular validation of conditionally replicative adenoviruses (CRAds)

All viruses were generated and plaque-purified in *E1*-complementing retinoblastoma 911 cells according to standard procedures. The CRAds were propagated in A549 adenocarcinoma cells. All viruses were purified by double cesium chloride ultracentrifugation (AdEasy system; QBiogene-MP, 11AES2016) and dialyzed against phosphate-buffered saline (Fisher Scientific, 20–012–027) with 10% glycerol. Viral particle titer for the purified preparations of each virus was determined by absorbance at 260 nm as described previously.[62] The absence of contamination with the wild-type *E1*A sequence-containing genomes (known as RCA) in virus preparations as well as genomic identity of each virus was verified by conventional PCR assays. Incorporation of pIX-mCherry fusion protein in the viral capsids and their molecular integrity was confirmed by western blot as using mouse monoclonal ANTI-FLAG® M2 (Sigma-Aldrich, F3165). Antibody binding was detected using the ECL™ chemiluminescence detection system (GE Healthcare, 45–002–401). Infectious titers were determined in HEK-293 helper cells by the 50% tissue culture infectious dose (TCID50) method. The limiting dilution end point and infectious titer (TCID50/ml) were determined by the Kärber equation: TCID50/ml = 10[1+D(S-0.5)]/V, where D is the logarithm of the dilution factor (e.g., D = 1 for the 10-fold serial dilution), S is the logarithm of the initial dilution plus the sum of ratios of infection-positive wells per total wells at each subsequent dilution, and V is the volume of the diluted vector, used for inoculation, in milliliters (ml).

Antibodies for immunoblotting, immunofluorescence and histology

The following primary antibodies were used for western blotting: rabbit anti-ATG5 (Cell Signaling Technology, 2630), anti-ATG7 (Cell Signaling Technology, 2613), anti-SQSTM1/p62 (Abcam, EPR4844), anti-LC3A/B (Novus Bio, NB100–233), anti-MMP14 (Abcam, AB38971), anti-MMP9 (Cell Signaling Technology, 2270) mouse anti-hexon (EMD Millipore, MAB8044), anti-GAPDH (EMD Millipore, MAB374); rabbit; for immunofluorescence: rabbit anti-KISS1 (Sigma-Aldrich, K0394), anti-BCL2 (Epitomics-Abcam, AP1303a), anti-CD24 (LSBio, c41096), anti-CD44 (Novus Bio, NBP1–41266) anti-CCL2 (GeneTex, GTX81767) anti-CXCL12 (LSbio, LS-c167170) and mouse FITC-labeled anti-FLOT2/ESA1 (GeneTex, GTX33201), anti-GFAP (Molecular Probes, A21282); and histology: rabbit anti-MMP9 (Novus Bio, NB110–57222) and mouse anti-KISS1 (clone 6a4.27) provided by D. R. Welch (KUMC).

Infection of BrCa cells

A) CN34Br or MDA-MB-231Br cells were labeled with premade lentiviruses expressing codon optimized *RFP* reporter under control of the *CMV* promoter (GenTarget Inc., LVP023).

B) *Rescue of stably-transfected BrCa cells with shRNA-silenced KISS1 gene expression.* The DNA sequence encoding shRNA for the human *KISS1* gene or scrambled shRNA was cloned into pLKO-based lentivirus vector (Sigma-Aldrich, SHCLNV-HM_002256) and MISSION *KISS1* shRNA lentiviral transduction particles were used. The MDA-MB-231Br cells were infected with either TRCN0000059067 (clone61) or TRCN0000059063 (clone79) lentiviral particles, which deliver shRNA against CDS of human *KISS1* gene (NM_002256) or Scrambled shRNA according to the protocol provided by the vendor and after 3 d subjected to puromycin selection in complete medium supplemented with 5 mg/ml of antibiotic (Invivogen, ant-pr-1) for 14 d. The level of *KISS1* knockdown was determined by quantitative RT-PCR.

C) *Generation of puromycin-resistant CN34Br cells expressing a* GFP-KISS1−*3′UTR reporter fusion.* Stable expression of *GFP-KISS1*−3′UTR reporter construct was achieved by using lentivirus-based vectors (Applied Biologicals Materials, MV-h61814) carrying *GFP* fused to 3′UTR region of the *KISS1* gene. Stable expression of Target cells plated in 96-well plate were infected with

the above lentiviruses and 24 h later virus-containing culture media was replaced with complete media supplemented with 1.2 μg/ml of puromycin. Puromycin-resistant clones were selected by culturing transfected cells for 2 wk under selective conditions.

Cell proliferation

MTT cell proliferation assay was performed according to the manufacturer's instruction for the Cell proliferation kit I (Roche, 11465007001). Results were expressed as a ratio between treated and untreated (mock) cells multiplied by 100%. Four wells were sampled as replicates per each experimental group in a given experiment. Data values are presented as means ± standard deviation.

Cell viability-calcein AM test

Cell membrane integrity was evaluated after transfection of cancer cells with siRNA, shRNA plasmids or infection with 1 multiplicity of infection of Ad or Ad-*KISS1* vectors by incubation of the cells with 2 μM calcein-AM. The assay was performed in 96-well plates as recommended by the vendor with 300 μl well volume (0.32 cm^2 growth area) and 100-μl sample volume per each well.

Boyden and Invasion assays

The migration property of MDA-MB-231Br based cells lacking *KISS1 (KISS1*-KD61, *KISS1*-KD79 or shScrambled) pretreated with mock, adenovirus (Ad) or Ad-*KISS1* vectors, 4T1Br-based transient transfected cells with *Kiss1*-KDA or shScrambled control was assessed using the Boyden assay. Briefly, 5×10^4 cancer cells were seeded in the top chamber of the BD cell migration system either covered (invasion test) or not covered with Matrigel (migration test;Trevigen, 3433–001–01). As a chemoattractant DMEM media supplemented with 10% FBS, serum-free DMEM (SF medium), normal astrocyte media (ScienCell, 1801) supplemented with astrocyte growth supplement (ScienCell, 1852) or astrocyte conditioned medium (ScienCell,1811-sf) supplemented with CXCL12/SDF1 (10 μg/ml; Peprotech, 300–28A) were used. Following a 24-h incubation, the number of migrating cells per field was counted using an Zeiss Axiovert 135 inverted microscope (Thornwood, NY, USA) at 10X magnification. A minimum of 8 images were collected and processed via MetaMorph software (Olympus, Japan).

Luciferase assay

MDA-MB-231Br cells were plated at a density of 5×10^4 cells per well in a 96-well plate 24 h before transfection. The next day, GoClone plasmids expressing fusion constructs of Luciferase reporter gene and the 3′UTR sequences containing either the *MIR345* binding site, mutated *MIR345* binding site or control vector were mixed (at a concentration of 30 ng/ml) with Gibco OPTI-MEM medium (Fisher Scientific, 31–985–062), *MIR345* mimic (SwicthGear Genomics, MIM0334), nontargeting (SwitchGear Genomics, MIM9001), and Fugene HD reagent (Promega, E2311) as per the protocol recommended by SwitchGear Genomics (Carlsbad, CA). After 30 min of incubation, 5 μl of transfection mixture was added to the each well. Cells were incubated for the next 48 h before measuring luciferase activity using a LightSwitch Assay kit (SwitchGear Genomics, LS010).

GFP analysis of KISS1 inhibition by MIR345-mimic

For analysis of GFP activity, CN34Br cells stable expressed GFP-KISS1−3′UTR fusion were plated in 24-well culture plate 24 h before treatment with NHA conditioned media alone or in combination with AMD3100, serum-free media supplemented with CCL2 or CXCL12, transfection with noncoding MIR-mimic (20 nM; GE Healthcare, CN-00100) or *MIR345*-mimic *(MIR345–5p*, 20 nM; GE Healthcare, c-300711) *MIR345*-mimic or nontargeting *MIR* mimic were delivered into target cells using DharmaFECT1 (GE Healthcare, T-2001). Activity of GFP expression was determined 48 h after transfection. From 5 to 8 GFP images were captured by phase-contrast fluorescent microscopy and signal intensity from region of interest (ROI) was assessed by ROI manager (ImageJ software).

Angiogenesis array

Semi-quantitative analysis of human cytokines was performed using a sandwich-based membrane-antibody array C1000 (AAH-ANG-1000) according to the vendor's recommendations (RayBiotech). Images were acquired with a Gel Doc XR System (Bio-Rad, Hercules, CA, USA) and analyzed relative to a positive control.

ELISA

Cells were seeded at the density of 50,000 cells per well 24 h before infection with a replication competent adenoviral vector expressing *KISS1* (Ad-*KISS1*) or an "unarmed" control vector (Ad). After 24 h of infection an unbound virus containing media was replaced with either a complete media or a serum-free medium (ELISA test) for the next 48 h of incubation. At 72 h post infection, supernatant from cells was harvested as per the manufacturer's instructions (KISS1 Enzyme Immunoassay Kit; Phoenix Pharmaceuticals Inc., EK-048–56). Detection of human KISS1 was performed by using biotinylated rabbit anti-KISS1 antibodies (Phoenix Pharmaceuticals Inc., EK-048–56) and streptavidin-horse radish peroxidase (HRP) conjugate (Phoenix Pharmaceuticals Inc., EK-SA-HRP). Signal was detected upon addition of the substrate solution (TMB; Phoenix Pharmaceuticals Inc., EK-SS) and measuring absorbance at 450 nm wavelength as per the vendor's protocol. Four wells were sampled per each experimental group and absorbance presented as mean ± standard deviation (SD).

Flow cytometry analyses

mCherry-positive CTCs were detected in the blood by flow cytometry using BD FACSAria Cell sorter (BD Biosciences, San Jose, CA). Blasticidin-resistant blood-derived MDA-MB-231

cells (CTC) were expanded and then stained with CD44, CD24 and EPCAM antibodies.[21]

Immunoblot analysis

Approximately 2 × 10^5 cells were lysed in 1X NP40 (Calbiochem, 492018)-based extraction buffer (20 mM HEPES, pH 7.9, 400 mM NaCl, 1 mM EDTA, 1 mM EGTA, 1% NP40, 1 mM DTT, 1 mM phenylmethylsulfonyl fluoride, 1 mg/ml aprotinin, 1 mg/ml leupeptin, 250 mg/ml benzamide, 50 mM NaF, and 1 mM NaO_3V_4) and Halt™ Protease Inhibitor Cocktail (Pierce-Thermo Scientific, 78429). Ten μg of total protein per sample was loaded onto a gel. After incubation with primary antibodies overnight, membranes were probed with either the secondary HRP goat anti-mouse antibody (Bio-Rad, 1721011), or HRP goat anti-rabbit antibodies (Bio-Rad, 1721019), and visualized with a Bio-Rad Imaging Station (Bio-Rad). Protein expression was quantified by band densitometry analysis using a Chemidoc Touch Imaging System (BioRad, Hercules, CA, USA) and data from 2 independent experiments were plotted vs housekeeping protein controls. Data were presented as fold change in protein expression level relative to that of the corresponding protein in scrambled shRNA construct-transfected cells.

RT-PCR and quantitative RT-PCR

A) *Detection of cellular mRNAs.* Extraction of total RNA from treated or untreated BrCa cells and human astrocytes was performed by using an RNeasy Mini Kit (Qiagen, 74104). Reverse transcription was performed using an iScript™ cDNA Synthesis kit (Bio-Rad, 1708890). Quantitative RT-PCR analysis was performed in triplicate by using the Power SYBR® PCR Master Mix (Applied Biosystems-Thermo-Fisher Scientific, 4368577) or iQ SYBR Green Supermix (Bio-Rad, 170–8880) according to the manufacturer's instructions, in a 10-μl reaction volume. Samples were run on a Bio-Rad Opticon II PCR station (Bio-Rad, Hercules, CA, USA) or ABI 7900HT Cycler (Applied Biosystems-Life Technologies,Waltham, MA). Expression levels were normalized to that of the human Actin (*ACTB*) gene. Amplification specificity was verified by melting curve analysis and agarose gel electrophoresis.

B) *Detection of cellular miRNAs.* Total RNA containing microRNA and mRNAs were extracted from formalin-fixed paraffin embedded tissue using an FFPE RNA extraction Kit (Qiagen, 73504) and from adherent cells using TRIzol reagent (Thermo Fisher Scientific, 15596026) according to the manufacturer's instructions. The quality of isolated RNA was determined with an Agilent and ND1000 Nanodrop Spectrophotometer (Nanodrop Technology-Thermo Scientific, Wilmington, DE, USA) before cDNA conversion using qScript miR cDNA Synthesis (Quanta Biosciences, 95107–100). The level of selective miRNAs expression was established by using PerfeCTa SYBR Green PCR SuperMix microRNA assay (Quanta Biosciences, 95053–500), miRNA specific assay (HSMIR-0345–5P) relative to cellular *RNU6–2* (HS-RNU6). The comparative ΔΔCt method was used to calculate the relative changes in gene expression by using an OPICON 2 Real time PCR machine (Bio-Rad).

Soft agar colony formation assay: In vitro tumorigenicity analysis

A methylcellulose colony formation assay was performed as described. Briefly, soft agar assays were performed by plating suspension of 1 × 10^4 cells in 1% low melting agarose. Cell colonies stained with 0.005% crystal violet colonies were counted 14 d later by drawing the grid on the plate. Experiments were repeated twice in triplicates.

Immunohistochemistry

Human brain or BrCa tissues were fixed overnight in 10% formalin solution (Thermo-Fisher Scientific, SF98–4). Five-micron-thick sections were deparaffinized, rehydrated and quenched in 1% hydrogen peroxide in methanol. Antigen retrieval was performed in 10 mM sodium citrate, pH 6.0, 0.1% Tween-20 (Fisher BioReagents, BP337–500). Blocking was done in 10% normal serum (Vector Laboratories, S-5000), 1% BSA (Sigma-Aldrich, A2153), and 0.1% Tween-20, followed by incubation with the primary antibodies diluted in 1% BSA overnight at 4°C. After incubating with secondary HRP-conjugated antibody, sections were developed with DAB Peroxidase (HRP) Substrate Kit (Vector Laboratories, SK-4100). Slides were counterstained with Gill's hematoxylin-eosin (Sigma-Aldrich, 1051740500), and mounted with Histomount (Fisher Scientific-National Diagnostics, 50–899–90137) before examination on a Zeiss AxioImager A2 microscope (Zeiss, Thornwood, NY).

Immunofluorescence

To determine the colocalization of CD24 and CD44, CCL2 and GFAP, CXCL12 and GFAP, EPCAM with CD44 and CD24, KISS1 with CD44 and GFAP markers, we performed immunofluorescent multicolor staining. Antigen retrieval was performed in citrate buffer, pH 6.0. The blocking step was performed by incubating the slides with Background Buster (Accurate Chemical & Scientific Corporation, NB306/50) and endogenous biotin activity was quenched followed by incubation with mouse antibody, rabbit antibody, or Alexa Fluor 488-labeled rabbit antibody (Novus Bio, NB110–89474AF488). The secondary biotinylated antibody (Vector Laboratories, BA-9200) treatment was followed by Streptavidin-Alexa Fluor 594 conjugate (Life Technologies – Molecular Probes, S32356). For negative controls the treatment was exactly the same except that the primary antibody was omitted. Slides were mounted in VECTASHIELD Antifade mounting medium containing DAPI (Vector Laboratories, H1200). Protein expression in tissue sections were visualized using a Leica SP5 AOBS Laser Scanning confocal microscope (Solms, Germany) with x90 (1,3 NA) or x60 (1.45 NA) oil objectives, or confocal images of immunofluorescently stained cells grown on coverslips were acquired with an Nikon Eclipse Ti-U microscope (Tokyo, Japan) and

images were captured by a Nikon digital sight DS-Qi1Mc camera, imported into and analyzed by IP Labs.

Orthotopic MDA-MB-231 BrCa model

The MDA-MB-231-mCherry model was established as described previously.[23] Fourteen, 28 and 42 d later, blood samples (1 ml) were collected from the heart, purified using GE Helathcare™ Percoll® centrifugation media (Fisher Scientific, 45–001–748) gradient centrifugation,[24] and cultured in medium containing 1 μg/ml blasticidin (Sigma-Aldrich, 203351). One wk later, Cherry-positive cells were subjected to flow cytometry using antibodies against CD24, CD44 and EPCAM markers. At 2, 4 and 6 wk post tumor implantation the number of mCherry-positive cancer cells was determined by Flow cytometry.

Statistics

All statistical analyses were performed using GraphPad Prism software. Statistical analysis of the data was performed using the Student unpaired *t* test, as indicated in the figure legends. A Log Rank test was using to compare the Kaplan-Meier survival curves. All experiments were performed twice and independently; *P* values <0.05 in all cases indicate statistical significance.

Abbreviations

3-Ma	3-methyladenine
aa	amino acid
BrCa	breast cancer
CSCs	cancer stem cells
CRAd	conditional replicated adenovirus
CTCs	circulating tumor cells
EGF	epidermal growth factor
EMT	epithelial-mesenchymal transition
FBS	fetal bovine serum
GAPDH	glyceraldehyde-3-phosphate dehydrogenase
GFAP	glial fibrillary acidic protein
GFP	green fluorescent protein
HR	homologous recombination
IL8	interleukin 8
IHC	immunohistochemical
kDA	kilodalton
MMP9	matrix metallopeptidase 9
RCA	replication competent adenovirus
ROI	region of interest
TMZ	temozolomide

Conflict of interest

Authors declare that they have no conflict of interest

Acknowledgments

This work was funded by Russian Fund of Fundamental Research (Russia), private donations and R03 CA102031 (AVB).

ORCID

Zaira Kadagidze http://orcid.org/0000-0002-0058-0987
Anatoly Baryshnikov http://orcid.org/0000-0002-2442-3011
Dmitry Malin http://orcid.org/0000-0002-5728-7511
Danny R. Welch http://orcid.org/0000-0002-1951-4947
Charles Cobbs http://orcid.org/0000-0001-7688-4293
Ilya V. Ulasov http://orcid.org/0000-0002-0818-0363

References

[1] Smid M, Wang Y, Zhang Y, Sieuwerts AM, Yu J, Klijn JG, Foekens JA, Martens JW. Subtypes of breast cancer show preferential site of relapse. Cancer Res. 2008;68:3108-14. doi:10.1158/0008-5472.CAN-07-5644. PMID:18451135

[2] Li F, Glinskii OV, Zhou J, Wilson LS, Barnes S, Anthony DC, Glinsky VV. Identification and analysis of signaling networks potentially involved in breast carcinoma metastasis to the brain. PLoS One. 2011;6:e21977. doi:10.1371/journal.pone.0021977. PMID:21779361

[3] Palmieri D, Smith QR, Lockman PR, Bronder J, Gril B, Chambers AF, Weil RJ, Steeg PS. Brain metastases of breast cancer. Breast Dis. 2006;26:139-47. doi:10.3233/BD-2007-26112

[4] Ohtaki T, Shintani Y, Honda S, Matsumoto H, Hori A, Kanehashi K, Terao Y, Kumano S, Takatsu Y, Masuda Y, et al. Metastasis suppressor gene KiSS-1 encodes peptide ligand of a G-protein-coupled receptor. Nature. 2001;411:613-7. doi:10.1038/35079135. PMID:11385580

[5] Zhang Y, Tang YJ, Li ZH, Pan F, Huang K, Xu GH. KiSS1 inhibits growth and invasion of osteosarcoma cells through inhibition of the MAPK pathway. Eur J Histochem. 2013;57:e30. doi:10.4081/ejh.2013.e30. PMID:24441183

[6] Cho SG, Yi Z, Pang X, Yi T, Wang Y, Luo J, Wu Z, Li D, Liu M. Kisspeptin-10, a KISS1-derived decapeptide, inhibits tumor angiogenesis by suppressing Sp1-mediated VEGF expression and FAK/Rho GTPase activation. Cancer Res. 2009;69:7062-70. doi:10.1158/0008-5472.CAN-09-0476. PMID:19671799

[7] Martin TA, Watkins G, Jiang WG. KiSS-1 expression in human breast cancer. Clin Exp Metastasis. 2005;22:503-11. doi:10.1007/s10585-005-4180-0. PMID:16320113

[8] McNally LR, Welch DR, Beck BH, Stafford LJ, Long JW, Sellers JC, Huang ZQ, Grizzle WE, Stockard CR, Nash KT, et al. KISS1 overexpression suppresses metastasis of pancreatic adenocarcinoma in a xenograft mouse model. Clin Exp Metastasis. 2010;27:591-600. doi:10.1007/s10585-010-9349-5. PMID:20844932

[9] Muir AI, Chamberlain L, Elshourbagy NA, Michalovich D, Moore DJ, Calamari A, Szekeres PG, Sarau HM, Chambers JK, Murdock P, et al. AXOR12, a novel human G protein-coupled receptor, activated by the peptide KiSS-1. J Biol Chem. 2001;276:28969-75. doi:10.1074/jbc.M102743200. PMID:11387329

[10] Navenot JM, Wang Z, Chopin M, Fujii N, Peiper SC. Kisspeptin-10-induced signaling of GPR54 negatively regulates chemotactic responses mediated by CXCR4: A potential mechanism for the metastasis suppressor activity of kisspeptins. Cancer Res. 2005;65:10450-6. doi:10.1158/0008-5472.CAN-05-1757. PMID:16288036

[11] Ulasov IV, Kaverina NV, Pytel P, Thaci B, Liu F, Hurst DR, Welch DR, Sattar HA, Olopade OI, Baryshnikov AY, et al. Clinical significance of KISS1 protein expression for brain invasion and metastasis. Cancer. 2012;118:2096-105. doi:10.1002/cncr.26525. PMID:21928364

[12] Stark AM, Tongers K, Maass N, Mehdorn HM, Held-Feindt J. Reduced metastasis-suppressor gene mRNA-expression in breast cancer brain metastases. J Cancer Res Clin Oncol. 2005;131:191-8. doi:10.1007/s00432-004-0629-9. PMID:15592684

[13] Gallagher PG, Bao Y, Prorock A, Zigrino P, Nischt R, Politi V, Mauch C, Dragulev B, Fox JW. Gene expression profiling reveals cross-talk between melanoma and fibroblasts: implications for host-tumor interactions in metastasis. Cancer Res. 2005;65:4134-46. doi:10.1158/0008-5472.CAN-04-0415. PMID:15899804

[14] Kim SJ, Kim JS, Park ES, Lee JS, Lin Q, Langley RR, Maya M, He J, Kim SW, Weihua Z, et al. Astrocytes upregulate survival genes in tumor cells and induce protection from chemotherapy. Neoplasia. 2011;13:286-98. doi:10.1593/neo.11112. PMID:21390191

[15] Abbott NJ. Astrocyte-endothelial interactions and blood-brain barrier permeability. J Anat. 2002;200:629-38. doi:10.1046/j.1469-7580.2002.00064.x. PMID:12162730

[16] Faulkner JR, Herrmann JE, Woo MJ, Tansey KE, Doan NB, Sofroniew MV. Reactive astrocytes protect tissue and preserve function after spinal cord injury. J Neurosci. 2004;24:2143-55. doi:10.1523/JNEUROSCI.3547-03.2004. PMID:14999065

[17] Kang Y, Siegel PM, Shu W, Drobnjak M, Kakonen SM, Cordon-Cardo C, Guise TA, Massagué J. A multigenic program mediating breast cancer metastasis to bone. Cancer Cell. 2003;3:537-49. doi:10.1016/S1535-6108(03)00132-6. PMID:12842083

[18] Sarvaiya PJ, Guo D, Ulasov I, Gabikian P, Lesniak MS. Chemokines in tumor progression and metastasis. Oncotarget. 2013;4:2171-85. doi:10.18632/oncotarget.1426. PMID:24259307

[19] Hwang-Verslues WW, Kuo WH, Chang PH, Pan CC, Wang HH, Tsai ST, Jeng YM, Shew JY, Kung JT, Chen CH, et al. Multiple lineages of human breast cancer stem/progenitor cells identified by profiling with stem cell markers. PLoS One. 2009;4:e8377. doi:10.1371/journal.pone.0008377. PMID:20027313

[20] Al-Hajj M, Wicha MS, Benito-Hernandez A, Morrison SJ, Clarke MF. Prospective identification of tumorigenic breast cancer cells. Proc Natl Acad Sci U S A. 2003;100:3983-8. doi:10.1073/pnas.0530291100. PMID:12629218

[21] Fillmore CM, Kuperwasser C. Human breast cancer cell lines contain stem-like cells that self-renew, give rise to phenotypically diverse progeny and survive chemotherapy. Breast Cancer Res. 2008;10:R25. doi:10.1186/bcr1982. PMID:18366788

[22] Zen K, Liu DQ, Guo YL, Wang C, Shan J, Fang M, Zhang CY, Liu Y. CD44v4 is a major E-selectin ligand that mediates breast cancer cell transendothelial migration. PLoS One. 2008;3:e1826. doi:10.1371/journal.pone.0001826. PMID:18350162

[23] Malin D, Strekalova E, Petrovic V, Deal AM, Al Ahmad A, Adamo B, Miller CR, Ugolkov A, Livasy C, Fritchie K, et al. alphaB-crystallin: a novel regulator of breast cancer metastasis to the brain. Clin Cancer Res. 2014;20:56-67. doi:10.1158/1078-0432.CCR-13-1255. PMID:24132917

[24] Shipitsin M, Campbell LL, Argani P, Weremowicz S, Bloushtain-Qimron N, Yao J, Nikolskaya T, Serebryiskaya T, Beroukhim R, Hu M, et al. Molecular definition of breast tumor heterogeneity. Cancer Cell. 2007;11:259-73. doi:10.1016/j.ccr.2007.01.013. PMID:17349583

[25] Corominas-Faja B, Cufi S, Oliveras-Ferraros C, Cuyas E, Lopez-Bonet E, Lupu R, Alarcón T, Vellon L, Iglesias JM, Leis O, et al. Nuclear reprogramming of luminal-like breast cancer cells generates Sox2-overexpressing cancer stem-like cellular states harboring transcriptional activation of the mTOR pathway. Cell Cycle. 2013;12:3109-24. doi:10.4161/cc.26173. PMID:23974095

[26] Bos PD, Zhang XH, Nadal C, Shu W, Gomis RR, Nguyen DX, Minn AJ, van de Vijver MJ, Gerald WL, Foekens JA, et al. Genes that mediate breast cancer metastasis to the brain. Nature. 2009;459:1005-9. doi:10.1038/nature08021. PMID:19421193

[27] Jaggupilli A, Elkord E. Significance of CD44 and CD24 as cancer stem cell markers: An enduring ambiguity. Clin Dev Immunol. 2012;2012:708036. doi:10.1155/2012/708036. PMID:22693526

[28] Liu S, Clouthier SG, Wicha MS. Role of microRNAs in the regulation of breast cancer stem cells. J Mammary Gland Biol Neoplasia. 2012;17:15-21. doi:10.1007/s10911-012-9242-8. PMID:22331423

[29] Rhodes LV, Bratton MR, Zhu Y, Tilghman SL, Muir SE, Salvo VA, Salvo VA, Tate CR, Elliott S, Nephew KP, et al. Effects of SDF-1-CXCR4 signaling on microRNA expression and tumorigenesis in estrogen receptor-alpha (ER-alpha)-positive breast cancer cells. Exp Cell Res. 2011;317:2573-81. doi:10.1016/j.yexcr.2011.08.016. PMID:21906588

[30] Kim SY, Lee CH, Midura BV, Yeung C, Mendoza A, Hong SH, Ren L, Wong D, Korz W, Merzouk A, et al. Inhibition of the CXCR4/CXCL12 chemokine pathway reduces the development of murine pulmonary metastases. Clin Exp Metastasis. 2008;25:201-11. doi:10.1007/s10585-007-9133-3. PMID:18071913

[31] Segatto I, Berton S, Sonego M, Massarut S, Fabris L, Armenia J, Mileto M, Colombatti A, Vecchione A, Baldassarre G, et al. p70S6 kinase mediates breast cancer cell survival in response to surgical wound fluid stimulation. Mol Oncol. 2014;8:766-80. doi:10.1016/j.molonc.2014.02.006. PMID:24661902

[32] Dutta C, Day T, Kopp N, van Bodegom D, Davids MS, Ryan J, Bird L, Kommajosyula N, Weigert O, Yoda A, et al. BCL2 suppresses PARP1 function and nonapoptotic cell death. Cancer Res. 2012;72:4193-203. doi:10.1158/0008-5472.CAN-11-4204. PMID:22689920

[33] Nihira K, Miki Y, Ono K, Suzuki T, Sasano H. An inhibition of p62/SQSTM1 caused autophagic cell death of several human carcinoma cells. Cancer Sci. 2014;105:568-75. doi:10.1111/cas.12396. PMID:24618016

[34] Wang Q, Jiang Z, Qi X, Lu S, Wang S, Leng C, Lu F, Liu H, Liang S, Shi J. Whole brain radiation therapy followed by intensity-modulated boosting treatment combined with concomitant temozolomide for brain metastases from non-small-cell lung cancer. Clin Transl Oncol. 2014;16:1000-5. doi:10.1007/s12094-014-1190-x. PMID:24894840

[35] Cho SG, Li D, Stafford LJ, Luo J, Rodriguez-Villanueva M, Wang Y, Liu M. KiSS1 suppresses TNFalpha-induced breast cancer cell invasion via an inhibition of RhoA-mediated NF-kappaB activation. J Cell Biochem. 2009;107:1139-49. doi:10.1002/jcb.22216. PMID:19533666

[36] Jiang Y, Berk M, Singh LS, Tan H, Yin L, Powell CT, Xu Y. KiSS1 suppresses metastasis in human ovarian cancer via inhibition of protein kinase C alpha. Clin Exp Metastasis. 2005;22:369-76. doi:10.1007/s10585-005-8186-4. PMID:16283480

[37] Li N, Wang HX, Zhang J, Ye YP, He GY. KISS-1 inhibits the proliferation and invasion of gastric carcinoma cells. World J Gastroenterol. 2012;18:1827-33. doi:10.3748/wjg.v18.i15.1827. PMID:22553409

[38] Yan C, Wang H, Aggarwal B, Boyd DD. A novel homologous recombination system to study 92 kDa type IV collagenase transcription demonstrates that the NF-kappaB motif drives the transition from a repressed to an activated state of gene expression. FASEB J. 2004;18:540-1. PMID:14715692

[39] Zheng S, Chang Y, Hodges KB, Sun Y, Ma X, Xue Y, Williamson SR, Lopez-Beltran A, Montironi R, Cheng L. Expression of KISS1 and MMP-9 in non-small cell lung cancer and their relations to metastasis and survival. Anticancer Res. 2010;30:713-8. PMID:20392988

[40] Jacob A, Jing J, Lee J, Schedin P, Gilbert SM, Peden AA, Junutula JR, Prekeris R. Rab40b regulates trafficking of MMP2 and MMP9 during invadopodia formation and invasion of breast cancer cells. J Cell Sci. 2013;126:4647-58. doi:10.1242/jcs.126573. PMID:23902685

[41] Hallett MA, Teng B, Hasegawa H, Schwab LP, Seagroves TN, Pourmotabbed T. Anti-matrix metalloproteinase-9 DNAzyme decreases tumor growth in the MMTV-PyMT mouse model of breast cancer. Breast Cancer Res. 2013;15:R12. doi:10.1186/bcr3385. PMID:23407024

[42] Rolli M, Fransvea E, Pilch J, Saven A, Felding-Habermann B. Activated integrin alphavbeta3 cooperates with metalloproteinase MMP-9 in regulating migration of metastatic breast cancer cells. Proc Natl Acad Sci U S A. 2003;100:9482-7. doi:10.1073/pnas.1633689100. PMID:12874388

[43] Tretiakova M, Kaverina N, Pytrl P, Kadagidze ZG, Barysnikov AY, Ulasov IV, Lesniak MS. Expression profile of matrix metalloproteinases in primary and metastatic breast cancer. Paper presented at 99TH Annual Conference USCAP; 2010 March 26; Washington, DC, USA.

[44] Cheng D, Kong H, Li Y. Prognostic value of interleukin-8 and MMP-9 in nasopharyngeal carcinoma. Eur Arch Otorhinolaryngol. 2014;271:503-9. doi:10.1007/s00405-013-2580-3. PMID:23749058

[45] Milovanovic J, Todorovic-Rakovic N, Abu Rabi Z. The prognostic role of interleukin-8 (IL-8) and matrix metalloproteinases -2 and -9 in lymph node-negative untreated breast cancer patients. J BUON. 2013;18:866-73. PMID:24344010

[46] Jovanovic M, Stefanoska I, Radojcic L, Vicovac L. Interleukin-8 (CXCL8) stimulates trophoblast cell migration and invasion by increasing levels of matrix metalloproteinase (MMP)2 and MMP9 and integrins alpha5 and beta1. Reproduction. 2010;139:789-98. doi:10.1530/REP-09-0341. PMID:20133364

[47] Lebrecht A, Grimm C, Lantzsch T, Ludwig E, Hefler L, Ulbrich E, Koelbl H. Monocyte chemoattractant protein-1 serum levels in patients with breast cancer. Tumour Biol. 2004;25:14-7. doi:10.1159/000077718. PMID:15192307

[48] Lu X, Kang Y. Chemokine (C-C motif) ligand 2 engages CCR2+ stromal cells of monocytic origin to promote breast cancer metastasis to lung and bone. J Biol Chem. 2009;284:29087-96. doi:10.1074/jbc.M109.035899. PMID:19720836

[49] Weiss JM, Cufi P, Bismuth J, Eymard B, Fadel E, Berrih-Aknin S, Le Panse R. SDF-1/CXCL12 recruits B cells and antigen-presenting cells to the thymus of autoimmune myasthenia gravis patients. Immunobiology. 2013;218:373-81. doi:10.1016/j.imbio.2012.05.006. PMID:22704519

[50] Cheng JW, Sadeghi Z, Levine AD, Penn MS, von Recum HA, Caplan AI, Hijaz A. The role of CXCL12 and CCL7 chemokines in immune regulation, embryonic development, and tissue regeneration. Cytokine. 2014;69:277-83. doi:10.1016/j.cyto.2014.06.007. PMID:25034237

[51] Qin H, Benveniste EN. ELISA methodology to quantify astrocyte production of cytokines/chemokines in vitro. Methods Mol Biol. 2012;814:235-49. doi:10.1007/978-1-61779-452-0_16. PMID:22144311

[52] Lee BC, Lee TH, Avraham S, Avraham HK. Involvement of the chemokine receptor CXCR4 and its ligand stromal cell-derived factor 1alpha in breast cancer cell migration through human brain microvascular endothelial cells. Mol Cancer Res. 2004;2:327-38. PMID:15235108

[53] Koyama Y, Kotani M, Sawamura T, Kuribayashi M, Konishi R, Michinaga S. Different actions of endothelin-1 on chemokine production in rat cultured astrocytes: Reduction of CX3CL1/fractalkine and an increase in CCL2/MCP-1 and CXCL1/CINC-1. J Neuroinflammation. 2013;10:51. doi:10.1186/1742-2094-10-51. PMID:23627909

[54] Wight RD, Tull CA, Deel MW, Stroope BL, Eubanks AG, Chavis JA, Drew PD, Hensley LL. Resveratrol effects on astrocyte function: Relevance to neurodegenerative diseases. Biochem Biophys Res Commun. 2012;426:112-5. doi:10.1016/j.bbrc.2012.08.045. PMID:22917537

[55] Jackson AL, Linsley PS. Recognizing and avoiding siRNA off-target effects for target identification and therapeutic application. Nat Rev Drug Discov. 2010;9:57-67. doi:10.1038/nrd3010. PMID:20043028

[56] Jackson AL, Bartz SR, Schelter J, Kobayashi SV, Burchard J, Mao M, Li B, Cavet G, Linsley PS. Expression profiling reveals off-target gene regulation by RNAi. Nat Biotechnol. 2003;21:635-7. doi:10.1038/nbt831. PMID:12754523

[57] Claerhout S, Verschooten L, Van Kelst S, De Vos R, Proby C, Agostinis P, Garmyn M. Concomitant inhibition of AKT and autophagy is required for efficient cisplatin-induced apoptosis of metastatic skin carcinoma. Int J Cancer. 2010;127:2790-803. doi:10.1002/ijc.25300. PMID:21351258

[58] Gupta P, Adkins C, Lockman P, Srivastava SK. Metastasis of breast tumor cells to brain is suppressed by phenethyl isothiocyanate in a novel metastasis model. PLoS One. 2013;8:e67278. doi:10.1371/journal.pone.0067278. PMID:23826254

[59] San Martin C, Glasgow JN, Borovjagin A, Beatty MS, Kashentseva EA, Curiel DT, Marabini R, Dmitriev IP. Localization of the N-terminus of minor coat protein IIIa in the adenovirus capsid. J Mol Biol. 2008;383:923-34. doi:10.1016/j.jmb.2008.08.054. PMID:18786542

[60] Shu X, Shaner NC, Yarbrough CA, Tsien RY, Remington SJ. Novel chromophores and buried charges control color in mFruits. Biochemistry. 2006;45:9639-47. doi:10.1021/bi060773l. PMID:16893165

[61] Ulasov IV, Borovjagin AV, Schroeder BA, Baryshnikov AY. Oncolytic adenoviruses: A thorny path to glioma cure. Genes Dis. 2014;1:214-26. doi:10.1016/j.gendis.2014.09.009. PMID:25685829

[62] Ulasov I, Borovjagin AV, Kaverina N, Schroeder B, Shah N, Lin B, Baryshnikov A, Cobbs C. MT1-MMP silencing by an shRNA-armed glioma-targeted conditionally replicative adenovirus (CRAd) improves its anti-glioma efficacy in vitro and in vivo. Cancer Lett. 2015;365(2):240-50. doi:10.1016/j.canlet.2015.06.002. PMID:26052095